

EM Undulator and Undulator A X-ray Profile Calculations for Grazing Incidence Insertion Device XBPM

Kenneth Schlax
Lee Teng Internship Program
University of Notre Dame

Advisor: Bingxin Yang
Argonne National Laboratory (ANL)
Advanced Photon Source (APS)
Accelerator Systems Division (ASD)
Diagnostics Group (DIAG)

August 13, 2010

Abstract

Recently we proposed a grazing-incidence insertion device x-ray beam position monitor (GRID-XBPM) for the APS front ends. We want to determine the appropriate XBPM aperture sizing given the design constraints to maximize transmission of central-cone monochromatic x-rays and to intercept a maximum amount of remaining x-ray power to facilitate center of mass (CM) beam position measurement. We calculated the monochromatic and total power x-ray profiles of Undulator A and the EM Undulator at 20-m from the source. We produced useful figures on transmission efficiency, beam widths, and signal flux over the range of operational gap settings. The result of this work was the production of two Tech Notes (DIAG-TN-2010-008[1], DIAG-TN-2010-010[2]). These tech notes provide information to the Diagnostics group, the users, and beam-line designers to facilitate informed conversation and decision making, not limited to aperture sizing but also as a contribution to a qualitative understanding of the x-ray beam properties.

Contents

1	Background and Motivation	3
1.1	Undulator Radiation	3
1.2	X-ray Beam Profiles	4
1.3	APS Structure	5
1.3.1	Undulators	5
1.3.2	XBPM and Beam Diagnostics	5
1.4	Introduction	6
2	Calculation Methods	6
3	Undulator A	6
4	EM Undulator	7
5	Conclusion and Future Work	9
6	Acknowledgments	10
	Appendix A: Undulator A Tech Note	11
	Appendix B: EM Undulator Tech Note	11

1 Background and Motivation

1.1 Undulator Radiation

Perpendicular acceleration to a relativistic moving charged particle generates synchrotron radiation. At such relativistic speeds, electrons in magnetic fields produce this radiation largely in a cone in their direction of travel. It is this relativistic focusing (in the observer’s frame) that makes synchrotron radiation an attractive source for high intensity radiation. Synchrotron radiation can be categorized by its source: bending magnets, wigglers, and undulators, in order of intensity magnification. Undulators produce exceptional brightness because, when compared to a bending magnet: Undulators with N -periods have $2N$ bending magnets, and the cone angular spread is compressed by a factor of \sqrt{N} . The result is an increase in x-ray intensity on the order of N^2 . [3] The undulator x-ray beam is practically divided into useful and expendible parts: the so-called monochromatic *central cone* and the wider-spread *white beam*. The central cone consists of coherent radiation at a wavelength determined by the physical environment of the undulator. The first harmonic energy of the undulator radiation is near a peak in the radiation spectrum.

$$\varepsilon_1[keV] = \frac{0.95E_e^2[GeV]}{(1 + K^2/2)\lambda_u[cm]} \tag{1}$$

$$\varepsilon_{peak} = \varepsilon_1(1 - 0.5/N) \tag{2}$$

The photons near peak flux are employed by most users in their experiments due to their high brightness and monochromaticity. Photons at other energies (white beam) are generally intercepted by a limiting aperture to reduce the load on the users optics. Another property of undulator radiation is polarization. Based on the configuration of the periodic undulator magnets, the x-ray beam can be both linearly and circularly polarized. Both the polarization and the monochromatic energies can be determined by examining what is called K -space.

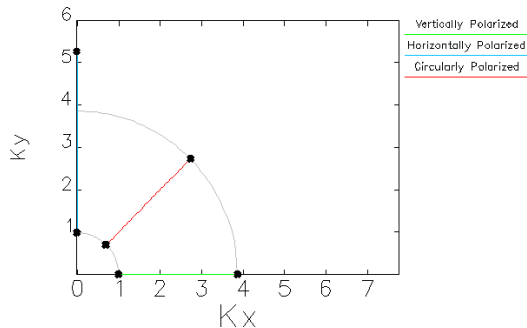
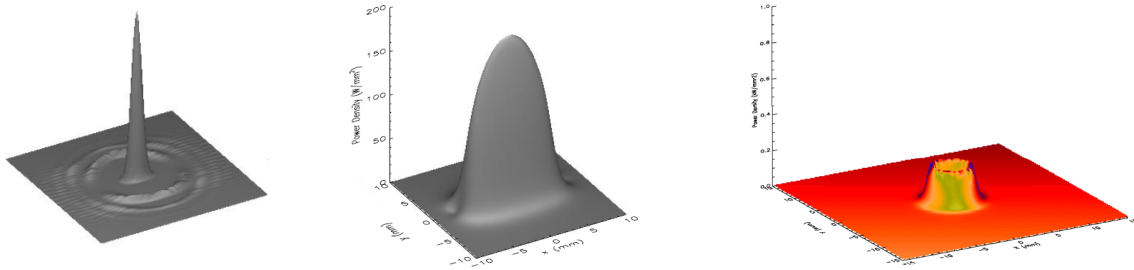


Figure 1: An example of K -space. Here the first harmonic energy and polarization of undulator radiation are represented by a vector with magnitude lying on a quarter circle of constant energy, and a direction indicating its degree of polarization. This example shows the range of possible polarizations and energies for the EM Undulator.

The expression K/γ is defined as the maximum slope of the transverse deflection caused by the undulator. Changing the undulator gap—the distance between the rows of periodic magnets—is the source of variable K . As the gap increases, K decreases, and the energy of the first harmonic, ω_1 increases. The range of K is limited by the physical space of the undulator.

Figure 2: Sample 3-D calculated x-ray distributions for: Central Cone, left [4]; Linearly Polarized Total Power, middle [4]; Circularly Polarized Total Power, right [5]



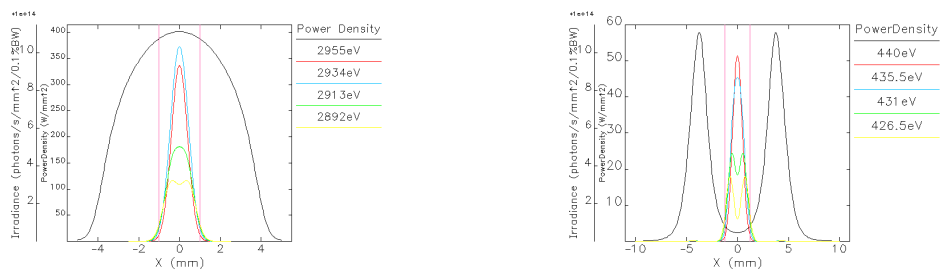
1.2 X-ray Beam Profiles

Moreover, changing the undulator gap changes the distribution and intensity of the white beam and monochromatic cone. Three dimensional distribution curves and two dimensional profiles can be used to display these effects. For linearly polarized x-rays, the undulator radiation intensity distribution (white beam) is gaussian. At a given gap setting, the total power x-ray distribution was found to be wider in the direction of polarization, and narrower in the perpendicular direction. As the gap is changed, the x-ray distribution is strongly affected in the polarized direction, while the x-ray distribution changes only slightly in the perpendicular direction. The perpendicular size is instead governed by the diffraction limit $\sqrt{\lambda/L}$. The white beam width and total power decreases with increasing gap.

In general, the distribution of monochromatic power is gaussian (at the first harmonic energy), but narrower than the total power. The central cone width decreases with increasing gap, but not as rapidly as the total power width decreases. The central cone width thus takes up an increasing percentage of the total power width as the gap is increased. The shape and intensity of the monochromatic energy changes significantly with undulator gap.

In circularly polarized cases, the total power distribution is non-gaussian. As K gets small, the two peaks of the total power profile merge and form a single peak, resembling very much a linearly polarized total power profile. This is likely due to the fact that at low K , the diffraction limit again is a significant factor, blending the weakly separated peaks. The central cone in the circular case behaves in the same way as in the linear case.

Figure 3: Sample x-axis monochromatic (color) and total power profiles for: Horizontally polarized Undulator A at $K_{y,max} = 2.747$ (left), Circularly polarized EM Undulator at maximum K , $K_x = K_y = 2.73$ (right)



1.3 APS Structure

The APS e^- storage beam passes through insertion devices (undulators, wigglers, or bending magnets), and the emitted synchrotron radiation is captured in a linear user beamline (called sectors). The x-ray beam lines contain many beam line optical devices, such as masks, shutters, filters, and x-ray beam position monitors (XBPMs), before the x-rays reach the experimental hall. This array of devices is called the *user front end*. For our purposes, we only need consider the undulator as insertion device and XBPM on the beam line.

1.3.1 Undulators

We considered two undulators, one in each tech note. The first we chose due to its prevalence: Undulator A is used in many beamlines. [5] Calculating the x-ray beam properties at a location in the front end is useful to beam designers and users, so that future designs and experiments can be based quantitatively on some of this work. It also served as a somewhat simpler case for calculations. The EM Undulator, on the other hand, is rare and complicated. [4] One is scheduled to be implemented in 2011. It can produce horizontally, vertically, and circularly polarized x-ray beams. Beam profile calculations will help not only in its implementation but also for understanding the characteristics of circularly polarized undulator radiation.

1.3.2 XBPM and Beam Diagnostics

The diagnostics group at the APS (ANL/APS/ASD/DIAG) is currently working on improving the x-ray beam position monitoring system. In preparation for the APS Upgrade, there is a desire to improve the accuracy of the x-ray beam position monitoring. This is critical because the APS is a feedback controlled system, so that the control and quality of the beam is only as good as it can be measured.

To that end, the diagnostics group is designing a grazing incidence insertion device x-ray beam position monitor (GRID-XBPM) as a part of the user front-ends.[6] There are two general approaches to measuring beam position: minimum sampling and centroid measurements. Using the former approach, XBPMs are designed to sample just the fringes of the white x-ray beam, reducing the load on the measurement device and the interference of the device on the beam. Sampling blades produce a current when impacted by the beam; the beam position can be deduced by comparing the currents vertically or horizontally. The latter approach, however, attempts to intercept as much of the beam as possible. To maintain the beam's usefulness, the amount of beam we can intercept is limited by the width of the useful central cone.

Blade XBPMs work well for linearly polarized x-ray beams, with a single peak. A difference in photoelectric current on two of the four symmetrical blades: top vs. bottom, left vs. right provides beam position information. However in circularly polarized cases, as found in the EM undulator, the total power distribution does not have a single peak, and thus the current comparison may be fooled.

The GRID-XBPM will necessarily then be of the centroid measurement type. We propose to combine the limiting aperture with the XBPM to intercept as much of the beam as practical. Combining the XBPM and the aperture has the advantage that misalignment between the two is no longer an issue. The XBPM is placed in grazing incidence because the expected power load is too great for a perpendicular slot XBPM. [7] A pinhole camera will then measure the x-ray fluorescence on the copper XBPM structure. The task ahead of us is to size an appropriate aperture given the design constraints to maximize transmission of central-cone monochromatic x-rays and to intercept a maximum amount of remaining x-ray power to facilitate center of mass (CM) beam position measurement.

1.4 Introduction

As a part of this effort we have calculated the total power and monochromatic beam profiles at the XBPM location. We have calculated and synthesized the beam size and transmission efficiency. We examined these beam properties over the ranges of expected operating conditions. We then discussed our calculations in the two tech notes, full of plots illustrating our calculated beam properties. These plots quantify what beam designers have a *feel* for and so provide them with the qualitative information needed to make a choice of aperture size. This work informs the discussion between accelerator scientists and beam users as to the appropriate balance between monochromatic transmission efficiency and sufficient signal flux. Ultimately an aperture size for each undulator/beamline must be chosen if the current XBPM design is to be implemented.

2 Calculation Methods

We used the program `xus` for the calculation of the undulator radiation. [8] The program was originally written by Roger Dejus, and later adopted for SDDS compatible input/output by Hairong Shang. SDDS stands for "self-described data sets". It includes a series of programs ranging from simple sorting algorithms to complex undulator radiation computations that manipulate data in columns and parameters, with labels and units included in the data itself. In this way data can be transferred between programs and manipulated into presentable forms. In the tech notes we calculated spectra and power density distributions using `sddsurgent -us`. Inputs to `sddsurgent` were properties of the e^- beam, the undulator parameter, number of periods, and gap setting, the distance to the location of interest, and the energy (range) of interest. The output from `sddsurgent` is an array of values of the intensity of x-rays at single points downstream from the undulator, either at a specific energy (for the monochromatic case), or a sum of all energies (for the total power case). These data points were then manipulated to derive distributions and trends of the undulator radiation at the location of interest. Programs to manipulate the `sddsurgent` calculations were written in `Tcl`, a shell scripting language, using other SDDS programs, such as `sddsplot`. We validated our SDDS results when possible using XOP, an interactive undulator radiation program.

3 Undulator A

Here we provide an analysis and summary of the calculations detailed in the tech note on Undulator A. The purpose of the tech note was to facilitate the aperture sizing of the GRID-XBPM to be placed on beamlines using Undulator A. The aperture as of now has been sized at 2-mm horizontally by 1.5-mm vertically. A rectangular aperture was chosen because Undulator A is only capable of producing horizontally polarized radiation. The width of the central cone is wider in the direction of polarization. We began these calculations by considering the range of conditions under which the XBPM would need to provide accurate measurements. This is qualified using the undulator parameter K . We determined that the range of K is between 2.747 and 0.4, with first harmonic energies ω_1 of 2955eV to 13056eV respectively. Varying energies are used for different experiments. The aperture size needs to be suitable for this range of energies. The following procedure was followed for maximum and minimum K cases:

We first plotted various useful energies around the first harmonic. These energies are abundant in the central cone, and are used by users more than other energies at a given K . These four selected energies near peak flux were used as reference for a central cone size. We calculated the total power and monochromatic profiles in the x and y directions. We also calculated the energy-integrated profiles of the same beam properties. These four

plots illustrate the x-ray beam size and distribution at the given K -value, and were used to get a general sense of the range of profile widths, and an idea of the region of a reasonable aperture size.

We then looked at the total power and monochromatic power as a single value integrated over various aperture sizes. This allowed a direct comparison between various monochromatic transmission efficiency cutoff levels (90%, 95%, 99%) and the amount of power that would be intercepted at those aperture cutoff levels.

After performing the above calculations for the maximum and minimum K cases, we then looked at the trends in total power width and monochromatic cutoff levels as a function of K between the extremes. This allows for fine tuning of the aperture size. Beam designers can see where exactly various amounts of monochromatic power are lost, and consult with the users to find a balance.

The calculations can be found Appendix A, the Undulator A tech note. The aperture was sized at 2.0-mm horizontally by 1.5-mm vertically. This permits 99% of the central cone to pass through the aperture in all but the closest gap settings. Even then the transmission efficiency is near 98 and thus the central cone is largely preserved under all gap settings.

Also of interest to beam users is the third harmonic photons. We looked at the third harmonic in the maximum K case. Compared with the first harmonic, the most notable difference is the presence of "wings" on the monochromatic central cone distribution. This means that an aperture needs to be wider if higher harmonics are going to be considered for the science being done on the beamline. We performed a similar series of calculations as on the maximum and minimum K cases.

4 EM Undulator

With a basis in our calculation method and analysis from looking at Undulator A, we set out to quantify the undulator radiation from the EM Undulator. The EM Undulator was more difficult to analyze because we had to consider the cases of horizontal, vertical, and circular polarization. We have noted the difference in trends of the circular versus linear polarization in the discussion of x-ray beam profiles (Sec 1.3). Because of the circular case, we need to size a square aperture for the EM Undulator. This immediately diminishes the sensitivity of the XBPM to either linear case.

The range of K -values went from 0.989 to 2.73 (Circular), 3.86(Vertical) and 5.27(Horizontal). This wider range of K values means that the widths of the central cone and total power profiles will vary more than in the Undulator A case. Indeed, examine the case of minimum versus maximum K at different polarizations. We need to choose one aperture size for these two extremes. Allowing 90%+ of the widest central cone case (Horiz. Max. K) means that we would transmit 2/3 or more of the total power in the smallest total power case (Vert. Min. K). Intercepting 50% of the smallest total power means that we also must intercept a significant portion of the widest central cone. Thus these calculations do not easily lend themselves to an appropriate aperture, but rather inform the beam designers and users that they must come to a compromise.

Finally we looked at signal flux. Because an aperture was not easily sized, it benefitted us to determine what and where sufficient x-ray fluorescence would be available. The spectrum of sufficiently energetic x-rays (i.e. $E \geq 9000$ eV) was plotted and integrated for various K -values in the region outside the aperture. We found that for most K , an aperture of 2.5-mm by 2.5-mm would be insufficient to distinguish the beam x-ray fluorescence photons from background photons originating in the storage ring bending magnets. This means that we will need to do more work to see if the aperture can be tightened or if the signal can be improved.

Figure 4: EM Undulator Horizontally Polarized Maximum K x-axis profile (left) and total power (right)

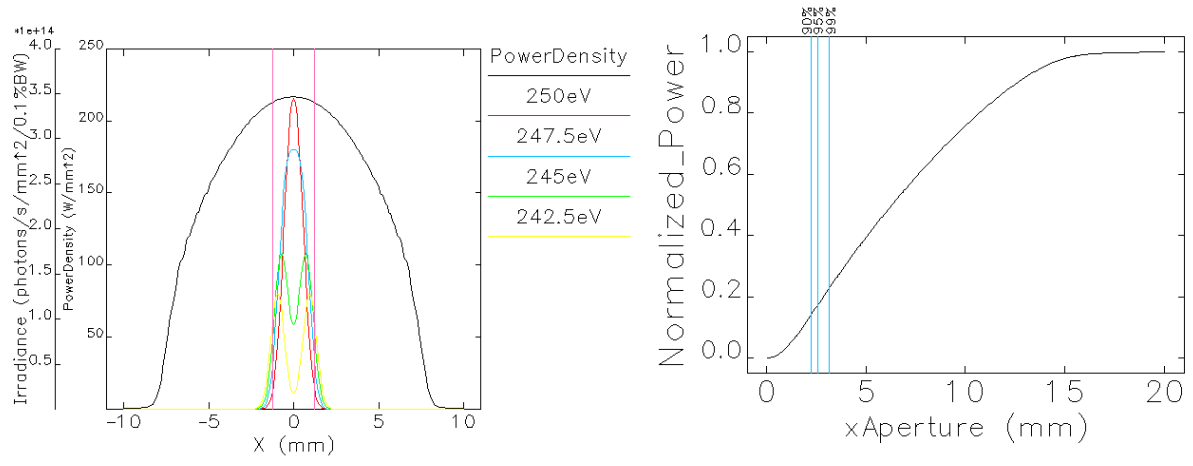
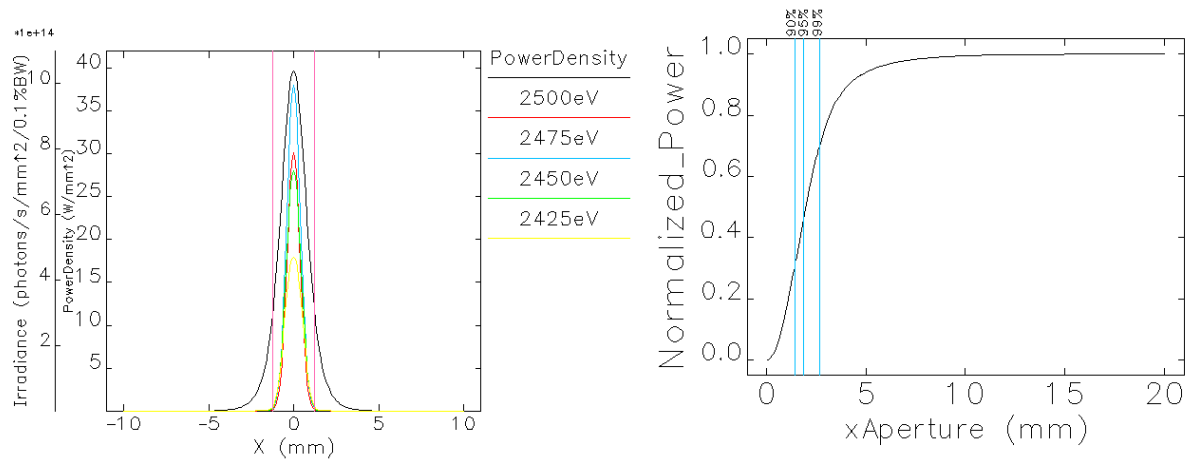


Figure 5: EM Undulator Vertically Polarized minimum K x-axis profile (left) and total power (right)



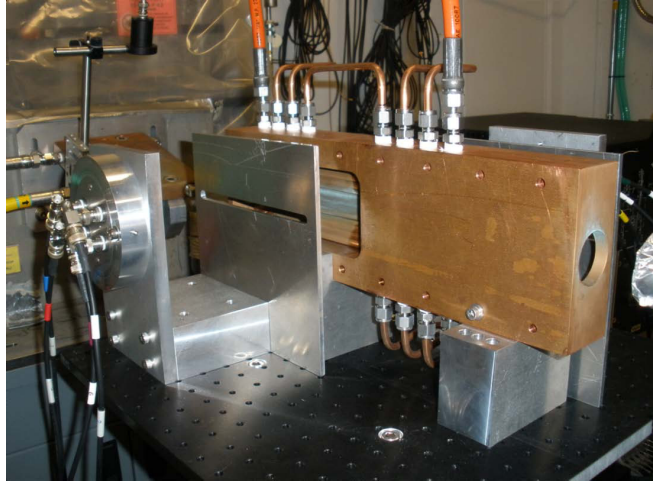


Figure 6: The prototype GRID-XBPM. The beam enters the hole at right, and impacts the grazing incidence copper inside. The x-ray fluorescence is detected by the pinhole camera at left. The prototype only measures in the vertical or horizontal direction. The actual XBPM will have two of these in series.

5 Conclusion and Future Work

The Undulator A aperture has been sized at 2-mm x 1.5-mm. The EM Undulator aperture has not yet been sized, but this work provides the information on which the beam designers and users will have to come to an agreement. We have further added to the understanding of the characteristics of undulator radiation from these two sources. We have established trends and fit equations to our calculations to determine the effect of the undulator settings on the downstream x-ray beam properties. These results are useful now in constructing the next generation of APS x-ray beam position monitors. The APS beam lines are feedback controlled systems. This means that the beams are only as good as the measurement systems from which feedback is obtained. Therefore quantitative information on the expected x-ray beam characteristics is important both in the design and operations phases of the APS. These results also thus are useful to future beam designers.

In the future, the diagnostics group intends on implementing the GRID-XBPM as part of the APS Upgrade. So far the XBPM has overcome the higher Upgrade beam power load. It has combined the aperture and the XBPM to eliminate misalignment between the two. This work has informed the choice of aperture size, and so a more precise aperture size may be chosen. A smaller aperture reduces the load on the users optics, facilitates shorter collimators and shutters, and reduces the downstream pipe diameter. A larger aperture means more x-ray intensity is available to the user, and thus better science can be done. It will be a balance between necessary signal flux and desired monochromatic efficiency.

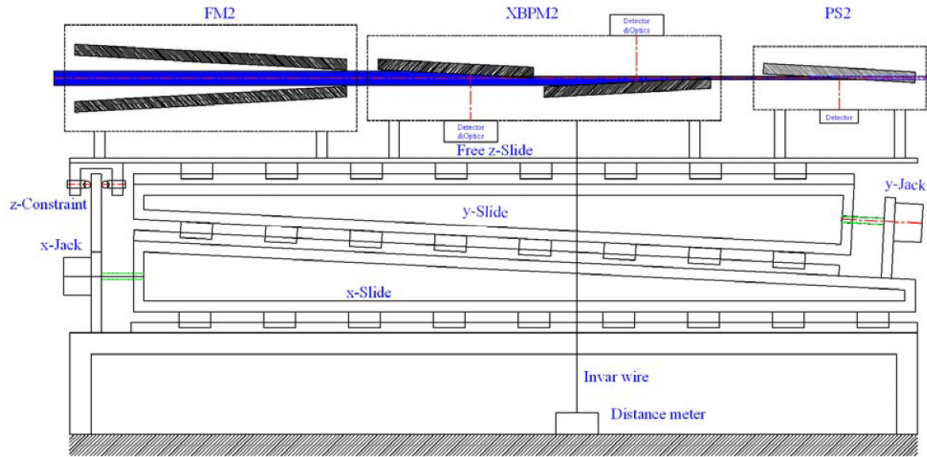


Figure 7: A schematic of the GRID-XBPM. The beam enters the left side, and is intercepted to produce x-ray fluorescence, all but for a small beam that passes through the aperture formed by the grazing incidence.

6 Acknowledgments

Bingxin Yang for his advice, insight, and work

GRID-XBPM Group for their consultation and conversation

Lee Teng Internship Program, for providing me with this opportunity

Linda Spentzouris for her efforts at ANL and the USPAS

Eric Prebys for his work with us and at FNAL

Argonne National Laboratory and Lisa Reed director of educational programs at ANL

References

- [1] B. Yang and K. Schlax, “Undulator-A x-ray profile calculations for grazing incidence XBPM design,” Tech. Rep. DIAG-TN-2010-008, Argonne National Laboratory, August 5, 2010.
- [2] B. Yang and K. Schlax, “IEX undulator x-ray profile calculations for grazing incidence XBPM design,” Tech. Rep. DIAG-TN-2010-010, Argonne National Laboratory, August 16, 2010.
- [3] K.-J. Kim, “Characteristics of synchrotron radiation,” *AIP Conference Proceedings*, vol. 184, no. 1, pp. 565–632, 1989.
- [4] R. Dejus, M. J. M. Group/ASD, and H. U. S. Sasaki Hiroshima Synchrotron Radiation Center, “On the selection of undulator for the IEX beamline: Power and spectral performance,” Tech. Rep. MD-TN-2009-003, Argonne National Laboratory, March 20, 2009.
- [5] R. Dejus, I. Vasserman, S. Sasaki, and E. Moog, “Undulator A magnetic properties and spectral performance,” Tech. Rep. ANL/APS/TB-45, Argonne National Laboratory, May, 2009.
- [6] G. Decker and B. Yang, “A concept for grazing incidenceXBPM in APS Front Ends,” Tech. Rep. DIAG-TN-2009-009, Argonne National Laboratory, October 18, 2009.
- [7] B. Yang, “Experimental test of a horizontal slot XBPM,” Tech. Rep. DIAG-TN-2009-006, Argonne National Laboratory, April 25, 2009.
- [8] M. S. del Rio and R. Dejus, “Status of XOP: an x-ray optics software toolkit,” *SPIE Proc.*, vol. 5536, pp. 171–174, 2004.

Appendix A:

DIAG-TN-2010-008

Undulator-A X-ray Profile Calculations for Grazing Incidence XBPM Design

Bingxin Yang, Argonne National Laboratory

Kenneth Schlax, University of Notre Dame

August 5, 2010

Work funded through:

Lee Teng Internship Program

A Joint Fermilab-Argonne-USPAS Program

Administered by the Illinois Accelerator Institute

Undulator-A X-ray Profile Calculations for Grazing Incidence XBPM Design

Bingxin Yang and Kenneth Schlax (July 15, 2010)

0. Abstract

Both monochromatic and energy-integrated x-ray profiles of Undulator A were calculated at 20-m from the source. A 2-mm \times 1.5-mm aperture allows more than 98% of the on-axis x-ray photons to pass through, for both monochromatic and pink x-ray beams of 1% bandwidth, while providing sufficient x-ray fluorescence for x-ray beam position monitors.

1. Background and motivation

Recently we proposed a grazing-incidence insertion device x-ray beam position monitor (GRID-XBPM) for the APS front ends [1,2]. The XBPM uses the fluorescence photons from the x-ray footprint on the limiting apertures to calculate the centroid of the undulator beam. In principle, the more x-ray photons we intercept, the better we can calculate the beam centroid. Beamline users normally need only x-ray photons in the monochromatic central cone. In this document, we calculate the monochromatic and energy-integrated x-ray profile width and height to facilitate the final choice of aperture dimensions of the XBPM.

2. Program for calculation of undulator radiation properties

We used the program *xus* for the calculation of the undulator radiation [3]. The program was originally written by Roger Dejus, and later adapted for SDDS compatible input/output by Hairong Shang [4]. Table 2-1 lists the undulator and beam parameters for the calculations. In this section, we calculated spectra and power density distributions using “*sddsurgent -us*” for the case of maximum K to illustrate the properties of the undulator radiation. Whenever possible, we also used XOP [5] in interactive mode to validate *sddsurgent*.

Choosing the maximum K parameter of Undulator A requires some thinking: An “average Undulator A” from 30 actual measurements in the APS [5] gives an effective field that results in $K_{\text{eff}} = 2.747$, and a peak field that gives $K_{\text{peak}} = 2.794$. The strongest device has $K_{\text{peak}} = 2.85$ [6]. If we calculate the peak intensity of the undulator footprint, it is best that the maximum peak field, or $K_{\text{max}} = 2.85$, is used. However, when we calculate the average profiles of the intensity distribution, the effective field is likely more suitable.

Figure 2-1 shows an angle-integrated spectrum of Undulator A at closed gap with $K_{\text{max}} = 2.76$. At this setting, the first harmonic photon energy ω_1 is 2933 eV, and the peak photon flux is found at photon energy approximately $0.75/N$ below ω_1 . A typical monochromatic x-ray user would set his monochromator within 2891 – 2912 eV, while a pink beam user will use photons between 2870 eV to 2912 eV, where the energy bandwidth $\Delta\omega/\omega$ is 1.5%.

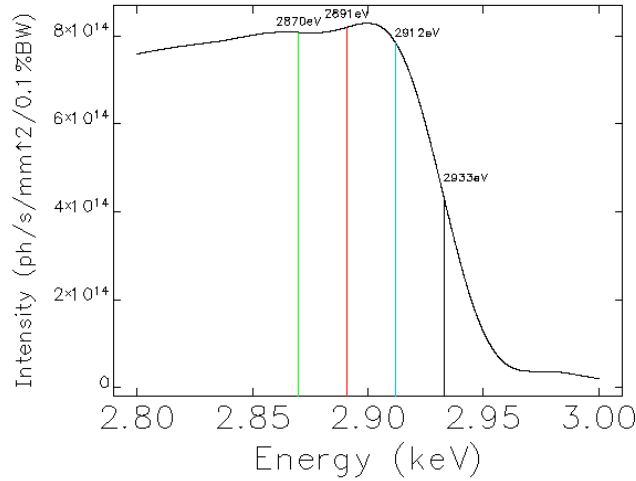


Figure 2-1: Monochromatic x-ray flux through a large pinhole at 20-m from Undulator A with $K = 2.76$ and the first harmonic energy of 2933 eV.

Table 2-1: Parameters used for undulator flux calculation

Quantity	Symbol	Values	Units	Notes
Undulator period	λ_u	3.3	cm	
Number of undulator periods	N	70		
Maximum K -value of Undulator A	K_{\max}	2.76		APS measurements [11]
Electron beam: horizontal size	σ_x	0.27	mm	Measured in Run 2010-1, validation of model [12].
Electron beam: vertical size	σ_y	0.012	mm	
Electron beam: horizontal divergence	$\sigma_{x'}$	0.012	mrad	
Electron beam: vertical divergence	$\sigma_{y'}$	0.004	mrad	

Figure 2-2 shows the Undulator A x-ray profiles measured along the x -axis: the total x-ray power profile, the monochromatic x-ray profiles at 2933 eV (first harmonic), 2912 eV (near peak flux), 2891 eV (near the cutoff for 1% BW), and 2870 eV (normally unused). The maximum flux in Figure 2-1 corresponds to photon energy slightly below ω_1 with a wider opening angle than at the first harmonic. If we set the horizontal aperture to 2 mm, as indicated by the vertical lines in Figure 2-2, most useful x-ray will pass through the aperture while most x-ray power will be intercepted by the aperture. The right panel of Figure 2-2 shows the vertically-integrated profiles of the same variables as plotted in the left panel. Here we can see that the relative intensities of the monochromatic x-ray lines have changed, but their profile widths have not changed significantly.

In a similar fashion, the left panel of Figure 2-3 shows the Undulator A x-ray profiles at $K_{\max} = 2.76$ measured along the y -axis, for the total x-ray power and the monochromatic x-ray photons at 2933 eV (first harmonic), 2912 eV (near peak flux), 2891 eV (near the cutoff for 1% BW), and 2870 eV (normally unused). If we set the vertical aperture to 1.5 mm, as indicated by the vertical lines in the figure, most useful x-ray photons will pass through while most power will be intercepted by the aperture. The right panel of Figure 2-3 shows the horizontally integrated profiles of the same variables as plotted in the left panel. Again, we can see that the

shape and relative intensities of the monochromatic x-ray lines changed noticeably, but their profile widths have not changed significantly. In both horizontal and vertical planes, the profiles in the symmetry plane do not differ greatly from the projected ones.

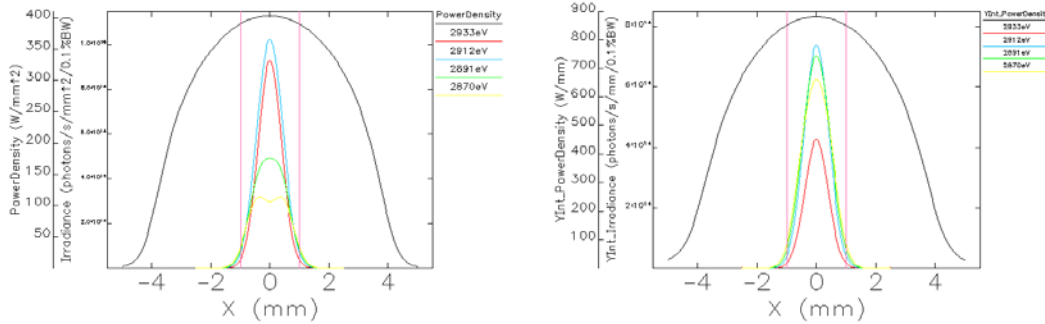


Figure 2-2: Calculated horizontal total x-ray power profiles of undulator A at 20 m from the source, along with monochromatic x-ray profiles at 2933 eV (first harmonic), 2912 eV, 2891 eV, and 2870 eV. The left panel shows the densities measured on the x -axis; and the right panel shows the vertically integrated power density.

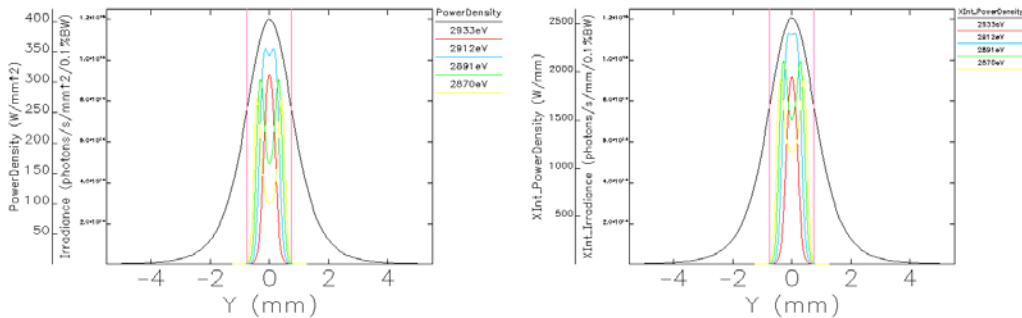


Figure 2-3: Calculated vertical total x-ray power profiles of undulator A at 20 m from the source, along with monochromatic x-ray profiles at 2933 eV (first harmonic), 2912 eV, 2891 eV, and 2870 eV. The left panel shows the densities measured on the y -axis; and the right panel shows the horizontally integrated power density.

Figure 2-4 shows the fraction of transmitted monochromatic x-ray photons within the central cone, plotted as a function of aperture (horizontal) width. The (vertical) aperture height is always assumed to be 75% of the width. Using the 2912-eV curve because it has the most photons in the central cone, we obtain three aperture sizes: 1.6 mm, 1.8 mm, and 2.2 mm, corresponding to 90%, 95% and 99% of transmission efficiency, respectively. Figure 2-5 shows the fraction of total x-ray power transmitted through the aperture plotted as a function of the aperture width, again with aperture height set at 75% of the width. We note that the same aperture that transmits 99% monochromatic photons at 2912 eV will intercept approximately 80% total x-ray power.

Many users use the third harmonic x-ray photons at the minimum gap. Figure 2-6 shows the angle-integrated spectrum of Undulator A at closed gap, $K = 2.76$ near its third harmonic photon energy $\omega_3 = 8800$ eV. Figure 2-7 shows the x-ray profiles in horizontal and vertical plane: the total x-ray power profile, the monochromatic x-ray profiles at 8800 eV (third harmonic), 8736 eV (near peak flux), 8643 eV (near the cutoff for 1% BW), and 8610 eV (normally unused).

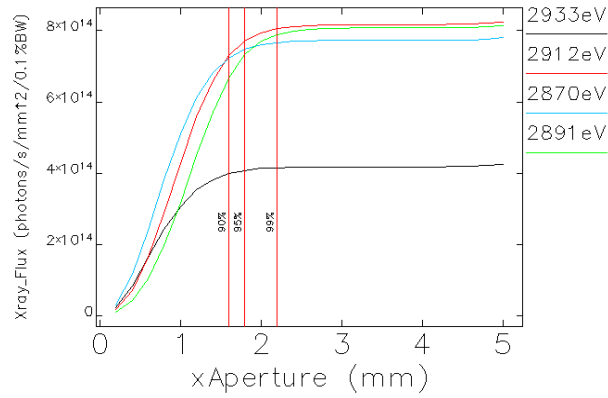


Figure 2-4: Monochromatic x-ray photon flux in the central cone plotted as a function of aperture width, for photon energies at and near the first harmonic. The aperture height is assumed to be 75% of the width.

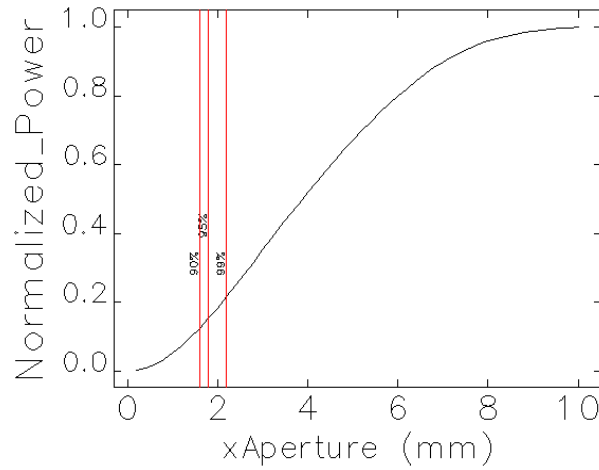


Figure 2-5: Transmitted x-ray power as function of aperture width. The aperture height is assumed to be 75% of the width.

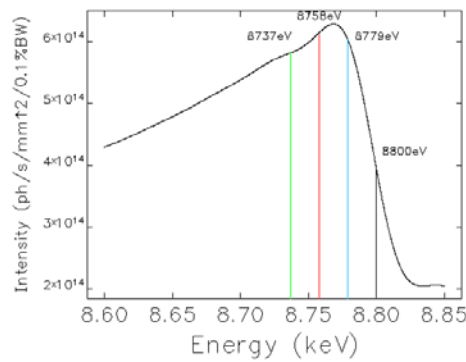


Figure 2-6: Monochromatic x-ray flux through a large pinhole at 20-m from Undulator A with $K = 2.76$ near its third harmonic energy of 8800 eV.

Figure 2-7 shows the Undulator A x-ray profiles measured along the x -axis: the total x-ray power profile, the monochromatic x-ray profiles at 8800 eV (third harmonic ω_3), 8779 eV (near peak flux), 8758 eV (near the cutoff for 1% BW), and 8737 eV (normally unused). A horizontal aperture of 2 mm, indicated by the vertical lines in the figure, allows most monochromatic x-ray photons in the central cone pass through, but not the ones in the side lobes. The right panel of Figure 2-7 shows the vertically-integrated profiles of the same variables as plotted in the left panel. Unlike the case of first harmonic, the projected intensity profiles have stronger side lobes than the profiles observed in the symmetry plane.

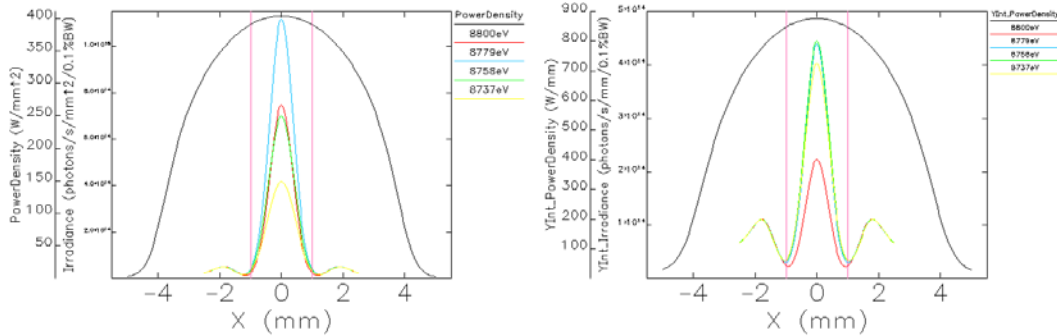


Figure 2-7: Calculated horizontal total x-ray power profiles of undulator A at 20 m from the source, along with monochromatic x-ray profiles at 8800 eV (third harmonic), 8779 eV, 8758 eV, and 8737 eV. The left panel shows the densities measured on the x -axis; and the right panel shows the vertically integrated power density.

In a similar fashion, the left panel of Figure 2-8 shows the Undulator A x-ray profiles at $K_{\max} = 2.76$ measured along the y -axis. If we set the vertical aperture to 1.5 mm, as indicated by the vertical lines in the figure, most useful x-ray photons will pass through. The right panel of Figure 2-8 shows the horizontally integrated profiles of the same variables as plotted in the left panel. Here we can see that the broad “background” intensities of monochromatic x-ray lines from the side lobes change noticeably, but their center peak widths have not changed significantly. In both horizontal and vertical planes, the specified aperture will let the entire center cone pass but block some x-rays from the side lobes.

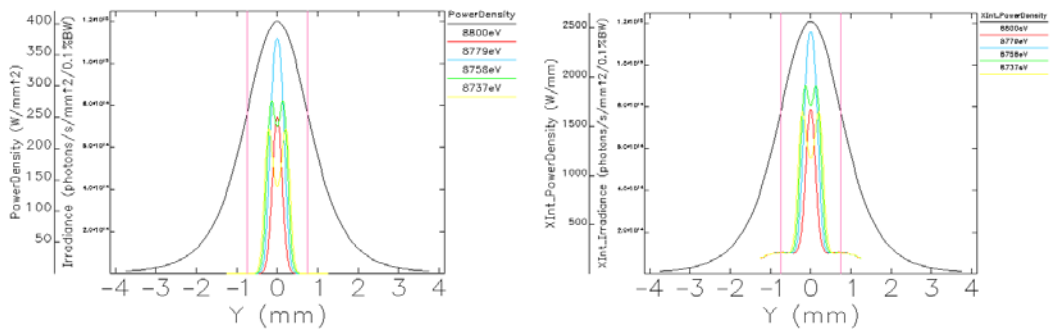


Figure 2-8: Calculated vertical total x-ray power profiles of undulator A at 20 m from the source, along with monochromatic x-ray profiles at x-ray profiles at 8800 eV (third harmonic), 8779 eV, 8758 eV, and 8737 eV. The left panel shows the densities measured on the y -axis; and the right panel shows the horizontally integrated power density.

3. Aperture compared with beam profiles at minimum K -values

During user operations, most beamlines using Undulator A run with the gap less than 30 mm, which we will take as the minimum gap for our design criteria, $G_{\min} = 30$ mm. The effective field data of thirty APS Undulators A was collected and averaged by Roger Dejus et al. [6]. Table 3-1 compares their measured Undulator A parameters at maximum and minimum gap settings.

Table 3-1: Comparison of Undulator A parameters at maximum and minimum gaps

Quantity	Symbol	Maximum	Minimum	Units
Undulator period length	λ_u	3.3		cm
Number of undulator periods	N	70		
Gap settings	G	10.5	30.0	mm
Peak undulator parameter K	K_{peak}	2.794	0.402	
Peak magnetic field	B_{peak}	0.9068	0.1304	T
Effective undulator parameter K	K_{eff}	2.747	0.404	
Effective magnetic field	B_{eff}	0.8915	0.1311	T

Figure 3-1 shows an angle-integrated spectrum of Undulator A with $K_{\min} = 0.40$. At this setting, the first harmonic photon energy ω_1 is 13056 eV, and the peak photon flux is found at photon energy approximately $0.75/N$ below ω_1 . A typical monochromatic x-ray user would set his monochromator within 12869 – 12953 eV, while a pink beam user could use photons between 12776 eV to 12953 eV, where the energy bandwidth $\Delta\omega/\omega$ is 1.5%.

The left panel of Figure 3-2 shows the projected horizontal x-ray profiles of Undulator A (or vertically-integrated profile) at $K_{\min} = 0.40$: the total x-ray power profile, the monochromatic x-ray profiles at 13056 eV (first harmonic), 12963 eV (near peak flux), 12869 eV (near the cutoff for 1% BW), and 12776 eV (normally unused). An aperture of 2 mm, indicated by the vertical lines, would allow most useful x-ray photons in the central cone to pass through while blocking most of the x-ray power. Similarly, the right panel of Figure 3-2 shows the projected vertical profiles (or horizontally-integrated profile) of the same undulator. Comparing Figure 3-2 with Figures 2-2 and 2-3, we note that in the horizontal plane, the monochromatic x-ray profiles do not change much with undulator gap, while the power profile changes significantly, since the former is determined largely by the horizontal e-beam divergence, while the latter is affected strongly by the K/γ ratio. In the vertical plane, on the other hand, the monochromatic x-ray profile is narrower for higher photon energy, $\sqrt{\lambda/2\pi L}$, at larger undulator gap, while the power profiles change less in relative terms.

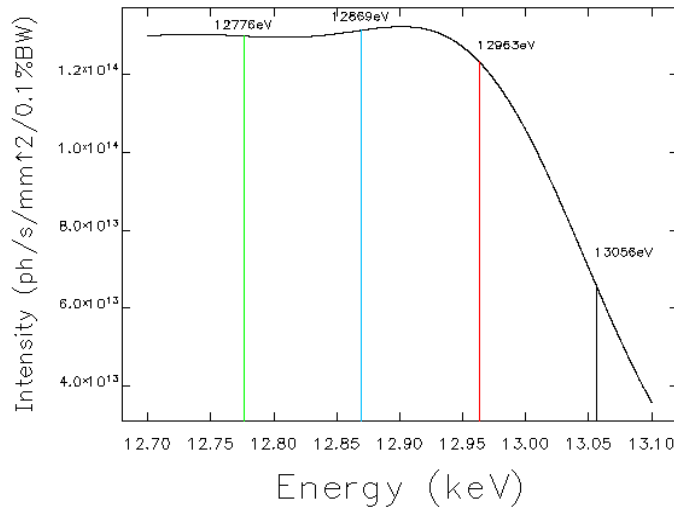


Figure 3-1: Monochromatic x-ray flux through a large pinhole at 20-m from Undulator A with $K = 0.40$ and the first harmonic energy of 13056 eV.

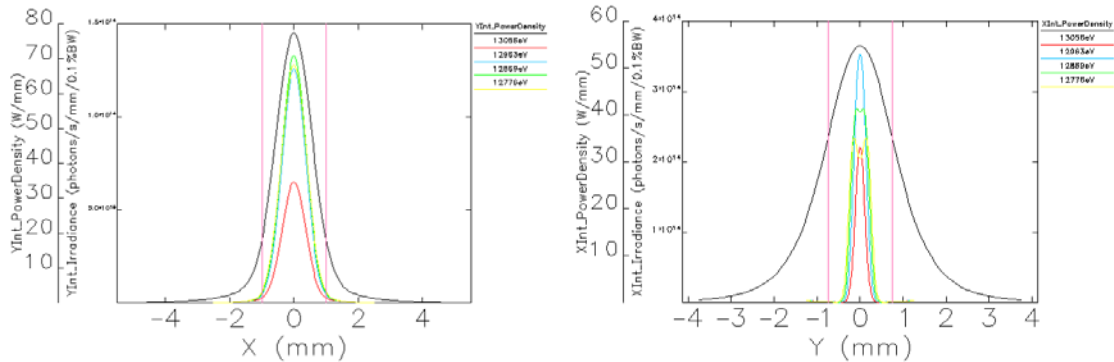


Figure 3-2: Projected horizontal (left) and vertical (right) total x-ray power profiles of undulator A at 20 m from the source, along with monochromatic x-ray profiles at 13056 eV (first harmonic), 12963 eV, 12869 eV, and 12776 eV.

Figure 3-3 shows the fraction of transmitted monochromatic x-ray photons within the central cone, plotted as a function of aperture (horizontal) width. The (vertical) aperture height is assumed to be always 75% of the width. Compared with Figure 2-4, the mono beam is more compact and 99% of it will pass the 2-mm \times 1.5-mm aperture. Figure 3-4 shows the fraction of total x-ray power transmitted through the aperture plotted as a function of the aperture width, again with aperture height set at 75% of the width. We note that the 2-mm \times 1.5-mm aperture intercepts about 50% of the total x-ray power. This should be sufficient to generate needed signals for beam position measurements. Since the total power is low with open gap, the downstream optics will not be overloaded even though the pass-through fraction is increased to 50%.

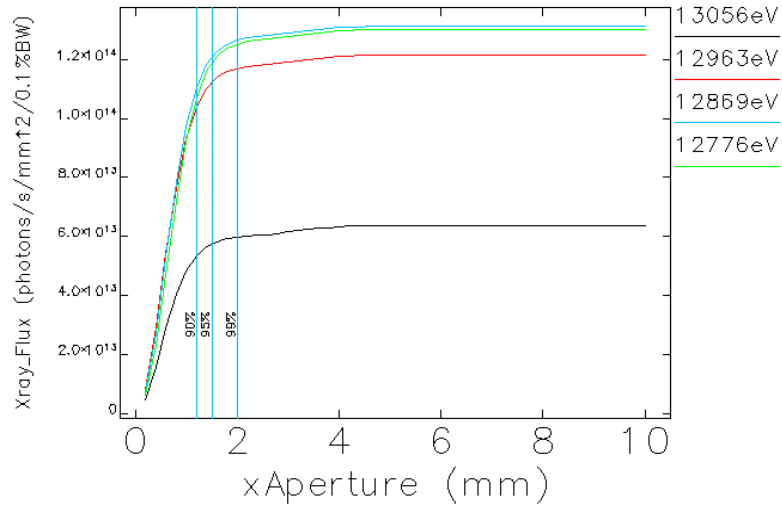


Figure 3-3: Monochromatic x-ray photon flux in the central cone plotted as a function of aperture width, for photon energies at and near the first harmonic. The aperture height is assumed to be 75% of the width.

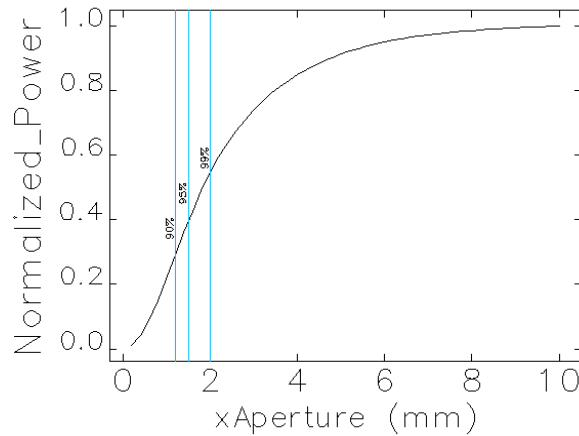


Figure 3-4: Transmitted x-ray power as function of aperture width. The aperture height is assumed to be 75% of the width.

4. Beam sizes for other gap settings

Figure 4-1 shows the average field data of thirty APS Undulator A over gap values 10.5 mm to 40 mm, collected by Roger Dejus et al. [7]. The data may be fitted to expressions of $R = G/\lambda_u$, where G is the undulator gap and λ_u is the undulator period length:

(1) linear fit,

$$B_{eff} [T] = 2.3990 \cdot \exp\{-3.1951 \cdot R\},$$

with an rms error of 0.84% and a maximum deviation of 3.6% for $10.5 \text{ mm} < G < 40 \text{ mm}$;

(2) quadratic fit,

$$B_{eff} [T] = 2.5657 \cdot \exp\{-3.3928 \cdot R + 0.1291 \cdot R^2\},$$

with an rms error of 0.33% and a maximum deviation of 0.93% for $10.5 \text{ mm} < G < 40 \text{ mm}$;
 (3) cubic fit,

$$B_{\text{eff}} [T] = 2.7948 \cdot \exp \left\{ -3.7860 \cdot R + 0.6808 \cdot R^2 - 0.2404 \cdot R^3 \right\},$$

with an rms error of 0.07% and a maximum deviation of 0.2% for $10.5 \text{ mm} < G < 40 \text{ mm}$.

In practice, the variations between undulators easily exceed the fitting errors, and the most accurate expressions are not necessarily more useful than the rough approximations.

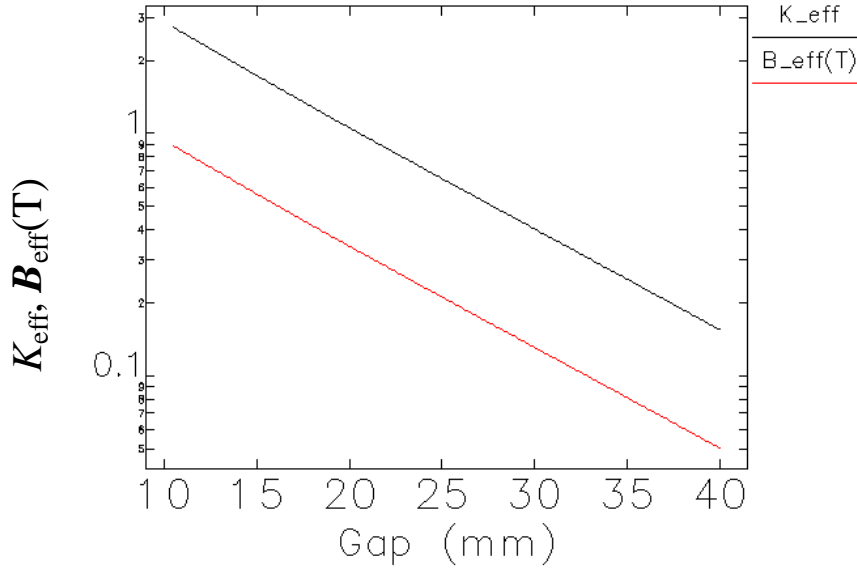


Figure 4-1: Measured undulator field data: average of 30 APS Undulators A [7].

The left panel of Figure 4-2 shows the horizontal and vertical beam sizes (FWHM) of the x-ray power profiles. As expected, the horizontal beam size W_x exhibits a strong dependence on undulator fields,

$$W_x = \frac{aS}{\gamma} \left(K^3 + b^3 \right)^{1/3}, \quad (1)$$

where the aperture distance, $S = 20 \text{ m}$ and the fit parameters $a = 1.67$ and $b = 0.46$. The right panel of Figure 4-2 shows the vertical beam size W_y , which is effectively independent of the undulator fields. The variation in the FWHM, of the order of 0.001 mm , is well below the grid size used in calculations determining the profile widths ($\Delta y = 0.0125 \text{ mm}$), and is deemed as insignificant.

Figure 4-3 shows the required aperture width to permit 90%, 95%, and 99% of the first harmonic monochromatic power through the aperture. As the gap increases, the first harmonic wavelength decreases, and the central cone size decreases. Only at the smallest gap settings is it calculated that slightly less than 99% of the monochromatic power passes through the proposed $2\text{-mm} \times 1.5\text{-mm}$ aperture.

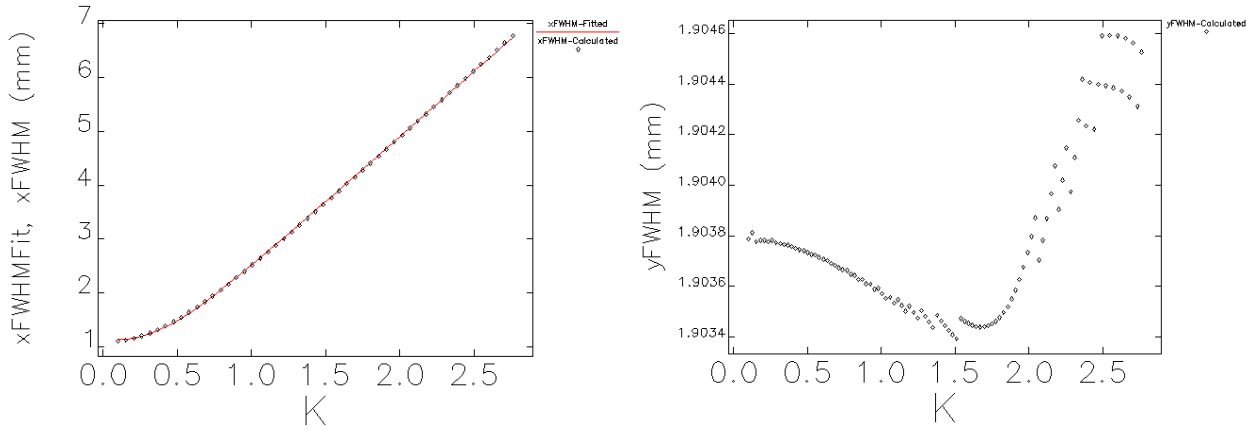


Figure 4-2: Projected horizontal and vertical profile sizes (FWHM) for Undulators A as a function of undulator field parameters.

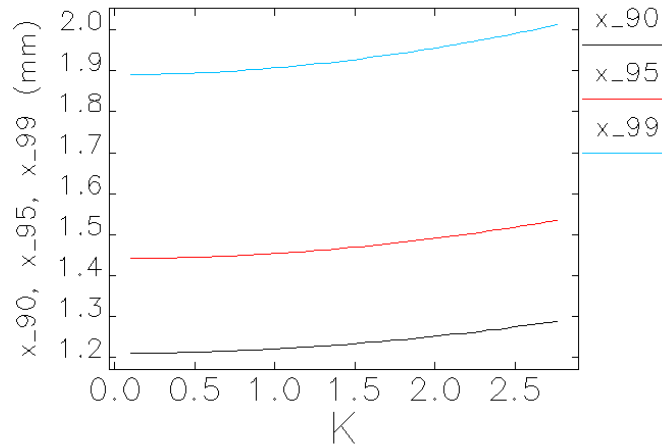


Figure 4-3: Required horizontal aperture size for transmitting 90%, 95%, and 99% of the radiation in the first harmonic central cone. The aperture height is assumed to be 75% of the width.

5. Discussions and conclusions

We calculated Undulator A x-ray beam profiles at 20 m from the source point, including the total power and the monochromatic central cone. For the energy-integrated x-ray beam, the horizontal beam size is mainly determined by K/γ , while the vertical beam size is independent of gap settings. For the monochromatic x-ray photons in the central cone, the horizontal beam size is mainly determined by the electron beam divergence, while the vertical beam size is largely determined by the diffraction limit, $\sqrt{\lambda/L}$. We found that more than 98% of the x-ray photons from the central cone will pass through the proposed aperture of 2 mm (H) \times 1.5 mm (V) at 20 m from the source for all undulator settings. Further tightening of the aperture is possible if users are willing to reduce the transmission efficiency in exchange for reduced power on the optics. The minimum acceptance aperture of the XBPM is determined by the maximum beam size at

maximum K -values. By inspecting Figures 2-2 and 2-3, we determined that a 10 mm \times 10 mm acceptance aperture would be needed for the GRID-XBPM (small dynamic range).

We would like to thank Roger Dejus for stimulating discussions about undulator radiation calculations and the results of Undulator A magnetic field measurements, Hairong Shang for her work of sdds-compatible version of urgent and her explaining of related programming issues. We would also like to thank Glenn Decker for his support for this project. One of us (KS) would like to thank the support of by the Lee Teng Undergraduate Internship in Accelerator Science and Engineering.

[References]

- [1] Bingxin Yang and Glenn Decker, A Concept for Grazing Incidence XBPM in APS Front Ends, APS/ASD/DIAG Technote DIAG-TN-2009-009.
- [2] B.X. Yang, G. Decker, S. H. Lee, and P. Den Hartog, High-power hard x-ray beam position monitor development at the APS, BIW10, Santa Fe, 2010.
- [3] M. Sánchez del Río and R. J. Dejus, "Status of XOP: an x-ray optics software toolkit," SPIE Proc. 5536, 171-174 (2004).
- [4] H. Shang, private communications.
- [5] XOP 2.3, ESRF web site, downloaded May 17, 2010.
- [6] R. Dejus, private communications.
- [7] R. Dejus et al., Undulator A measurements, private communications.

Appendix A: Notes on undulator radiation programs XOP and sddsurgent

In this work, we used programs xus in the XOP suite and sddsurgent for calculate the undulator radiation. Here are some cautionary notes on the use of these programs, as of July 2010.

A.1 Power profiles

When calculating the total power profiles using xus and “sddsurgent -us”, we discovered anomalies in the profile shapes for calculation method is chosen as finite-N, non-zero emittance. For example, in the left panel of Figure A-1, there is a small bump at the peak of the horizontal power profile. The right panel, calculated power profile for similar undulator settings, but with zero emittance, does not show this anomaly. The problem appears to be in the convolution function in the program. Roger Dejus [A-1], author of the xus program, suggested that we use the zero emittance for all power profile calculation. Following his advice, all power profiles shown in this note were calculated assuming zero emittance. The monochromatic radiation profiles, on the other hand, were calculated using non-zero emittance.

To double check the power calculation, we numerically integrated the power profile over the entire aperture. The integration yielded $P_T = 5.66$ kW for maximum K_{eff} . Using the closed-form expression [A-2],

$$P_T[kW]= 0.633 E^2[GeV]B_0^2[T]L[m]I[A] ,$$

we obtained $P_T = 5.80$ kW. The agreement between the two is within 2.5%.

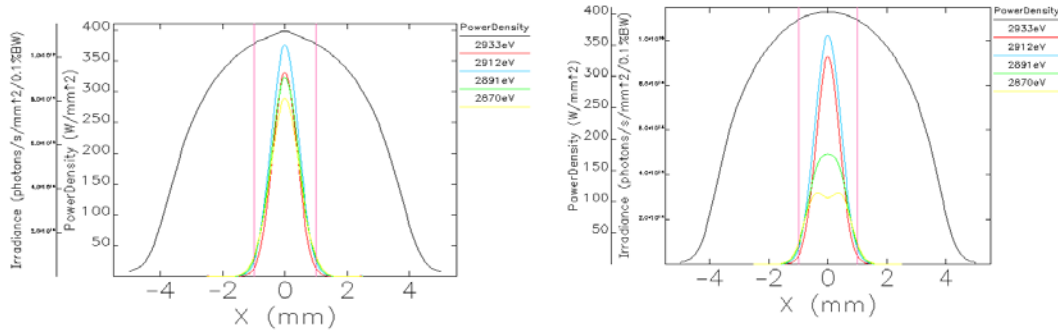


Figure A-1: The left panel shows the incorrect total power density profile using “sddsurgent -us -calculation=mode=powerDensity,method=Dejus”. The right panel shows the version we used: “sddsurgent -us -calculation=mode=powerDensity,method=WalkerFinite”

A.2 FWHM of the power profile

The plots of the horizontal and vertical beam size (Figure 4-2) can perhaps be made more sensible by looking also at Figure A-2. The left panel shows that as K increases, the horizontal size increases. The right panel, on the other hand, shows that the vertical size is effectively constant for different K . If we were to draw a vertical line at about ± 0.95 mm, we would approximately intercept the curves at their FWHM for all K .

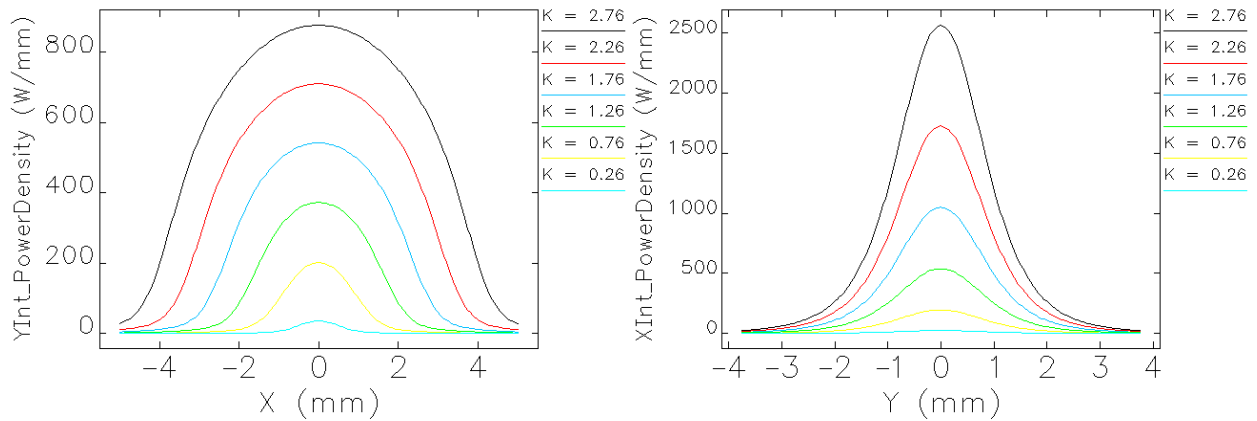


Figure A-2: Horizontal and vertical beam sizes at several K -values. Notice how the horizontal beam size increases with K -value, while the vertical size remains relatively constant.

[A-1] M. Sánchez del Río and R. J. Dejus, "Status of XOP: an x-ray optics software toolkit," SPIE Proc. 5536, 171-174 (2004).

[A-2] Janos Kirz, et al., "X-ray data booklet."

Appendix B:

DIAG-TN-2010-010

IEX Undulator X-ray Profile Calculations for Grazing Incidence XBPM Design

Bingxin Yang, Argonne National Laboratory

Kenneth Schlax, University of Notre Dame

August 16, 2010

Work funded through:

Lee Teng Internship Program

A Joint Fermilab-Argonne-USPAS Program

Administered by the Illinois Accelerator Institute

IEX Undulator X-ray Profile Calculations for Grazing Incidence XBPM Design

Bingxin Yang and Kenneth Schlax (August 15, 2010)

0. Abstract

We calculated monochromatic and energy-integrated x-ray profiles of electromagnetic undulator (EMU) for Intermediate Energy X-ray (IEX) beamline, Sector 29, at 20-m from the source. A square aperture of 2.5 mm is proposed for the GRID-XBPM to allow 90% - 99% of monochromatic x-ray photons in the central cone to pass through. For horizontal placement of GRID-XBPM plates, the strongest XBPM signal is found in 250-eV horizontal linear polarization operation mode, while the weakest signal is for 2500-eV vertical linear polarization mode. The intensity ratio of these signals is 3×10^4 . A smaller aperture is desired.

1. Background and motivation

Recently we proposed a grazing-incidence insertion device x-ray beam position monitor (GRID-XBPM) for the APS front ends [1, 2]. The XBPM uses the fluorescence photons from the x-ray footprint on the limiting apertures to calculate the centroid of the undulator beam. Beamline users normally need only x-ray photons in the monochromatic central cone. In principle, the more x-ray photons we intercept outside the central cone, the better we can measure the beam centroid. In a related tech note, we calculated the monochromatic and energy-integrated x-ray beam profiles of Undulator A to facilitate the final choice of XBPM aperture dimensions [3]. In this document, we perform similar calculations for the elliptically polarized EM undulator to be installed in Sector 29, the intermediate energy x-ray (IEX) beamline.

The choice of the electro-magnetic undulator (EMU) for the IEX was discussed in detail by R. Dejus, M. Jaski and S. Sasaki [4], which has been slightly modified [5]. Table 1-1 lists the basic parameters relevant to these calculations. Comparing with the popular Undulator A used by most APS user beamlines, the IEX-EMU's first harmonic photon energy reaches down to 250 eV. This fact has important implications for the GRID-XBPM design:

- (1) Wide monochromatic central cone: At the closed gap, the maximum photon wavelength is 4.96 nm and the central cone radius is $\sqrt{\lambda_{1,\max} / 2L} = 22.9 \mu\text{rad}$. This is more than doubling that of Undulator A, $\left[\sqrt{\lambda_{1,\max} / 2L} \right]_{UA} = 9.2 \mu\text{rad}$, and is comparable to the power cone radius $0.4/\gamma = 29 \mu\text{rad}$. The wide central cone significantly influences our choice of XBPM aperture.
- (2) Aperture aspect ratio: Since the monochromatic central cone at the first harmonic is nearly as wide as the horizontal e-beam divergence, the x-ray beam radii below the harmonic photon energy will be even wider. As a result, the photon beam cross section is more circular and less ribbon-like; and our XBPM aperture will have an aspect ratio of 1:1 instead of 4:3 for Undulator A.

(3) The maximum value of the first harmonic photon energy, $\omega_{1,\max} = 2\gamma^2\omega_u = 3.72$ keV, is well below 8.979 keV, the K absorption edge of Cu. Unlike Undulator A, which has $[\omega_{1,\max}]_{UA} = 14.7$ keV, and generates x-ray fluorescence (XRF) photons even at low- K settings, the IEX-EMU will not produce measurable Cu- K XRF until it generates sufficient third harmonic x-ray photons for off-axis detection. For this reason, we arbitrarily take $K_{\min} = 0.989$ as our minimum K value, for which $\omega_1(K_{\min}) = 2500$ eV. Its fifth and higher harmonics may be used by the Cu-based GRID-XBPM.

Table 1-1: Key parameters of the EM undulator for the APS IEX beamline [4, 5]

Quantity	Symbol	Values			Units
		Horizontal	Vertical	Circular	
Undulator period	λ_u	12.5			cm
Number of undulator periods	N	38			
Undulator length	L	4.75			m
Maximum horizontal K	$K_{x,\max}$	0	3.86	2.73	
Maximum vertical K	$K_{y,\max}$	5.27	0	2.73	
Minimum first harmonic energy	$\omega_{1,\min}$	250	440	440	eV
Minimum horizontal K	$K_{x,\min}$	0	1.0	0.699	[*]
Minimum vertical K	$K_{y,\min}$	0.989	0.989	0.699	[*]
Minimum first harmonic energy	$\omega_{1,\max}$	2500	2500	2500	eV
Maximum total power	P_T	6.0	3.2	3.2	kW
Maximum on-axis power density		89	65	1	kW/mrad ²
E-beam horizontal size	σ_x	0.27			Mm
E-beam vertical size	σ_y	0.012			Mm
E-beam horizontal divergence	$\sigma_{x'}$	0.012			Mrad
E-beam vertical divergence	$\sigma_{y'}$	0.004			Mrad

[*] See discussion in the main text for “minimum” K -values.

We used the program xus for the calculation of the undulator radiation [6]. The program was originally written by Roger Dejus, and later adapted for SDDS compatible input/output by Hairong Shang [7]. Whenever possible, we will use XOP [8] in interactive mode to validate the program sddsurgent.

Figure 1-1 shows the parameters space in (K_x, K_y) plane defined by Table 1-1 [4, 5]: The maximum K -values are defined by a quarter circle, $K_x^2 + K_y^2 = 14.9$; the minimum K -values are defined by another quarter circle, $K_x^2 + K_y^2 = 0.978$; and the additional K -range for horizontal polarization where $K_{y,\max} = 5.27$. In the next three sections, we will discuss cases for these three polarizations separately.

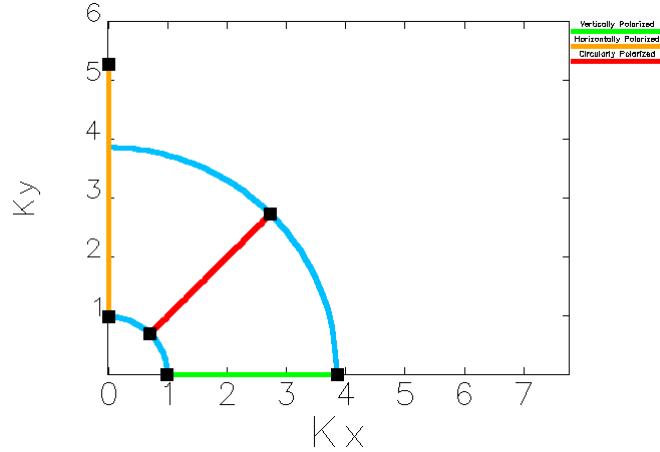


Figure 1-1: K -space for the IEX-EM undulator used for this calculation: operation with horizontal polarization is shown in the vertical line, $0.989 \leq K_y \leq 5.27$; operation with vertical polarization is shown in the horizontal line, $0.989 \leq K_x \leq 3.86$; operation with circular polarizations is shown in the diagonal line; and operation with elliptical polarizations are shown in the area between the two quarter circles, $0.978 \leq K_x^2 + K_y^2 \leq 14.9$.

2. Horizontally polarized undulator beam properties

In this section, we calculate spectra and power density distributions for beams with linear polarization in the horizontal plane and compare the patterns with a proposed aperture.

2.1 Maximum K for horizontally polarized x-rays

Figure 2-1 shows an angle-integrated spectrum of IEX-EM undulator for $K_{y,max} = 5.27$. At this setting, the first harmonic photon energy ω_1 is 250 eV. The monochromator x-ray user would set his monochromator near the peak of photon flux at approximately 245 eV.

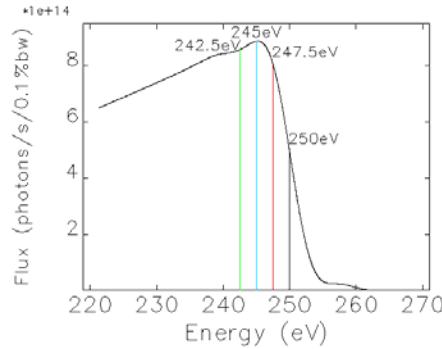


Figure 2-1: Monochromatic x-ray flux through a $5 \text{ mm} \times 5 \text{ mm}$ aperture which encloses the central cone at 20-m from IEX-EM Undulator with $K_y = 5.27$ and $\omega_1 = 250 \text{ eV}$.

Figure 2-2 shows the IEX-EMU beam profiles measured along the x -axis (left panel) and y -axis (right panel): the total x-ray power profile, the monochromatic x-ray profiles at 250 eV (first harmonic), 247.5 eV, 245eV (spectral peak), and 242.5 eV (normally unused). The maximum flux in Figure 2-1 corresponds to photon energy slightly below ω_1 with a wider opening angle

than the harmonic. If we set the horizontal and vertical apertures to 2.5 mm, as indicated by the vertical lines in both panels of Figure 2-2, most useful x-ray photons will pass through the aperture while most x-ray power will be intercepted.

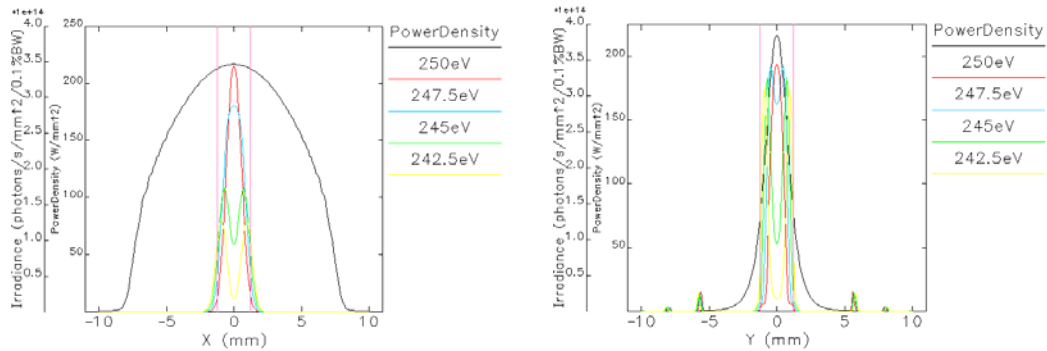


Figure 2-2: Calculated x-ray beam profiles of IEX-EM undulator at maximum K along the horizontal (left panel) and vertical (right panel) symmetry axis. The observation plane is 20 m from the source. The data includes total x-ray power profile, and monochromatic x-ray profiles at 250 eV (first harmonic), 245 eV, 247.5 eV, and 242.5 eV.

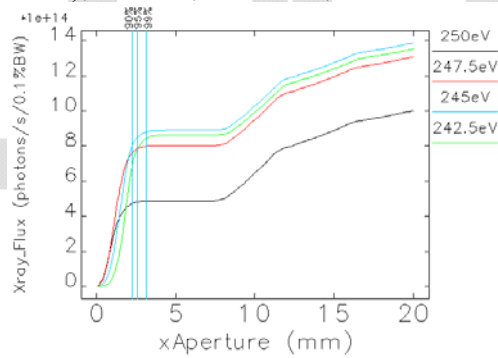


Figure 2-3: Monochromatic x-ray photon flux in the central cone plotted as a function of sides of square beam aperture, for photon energies at and near the first harmonic.

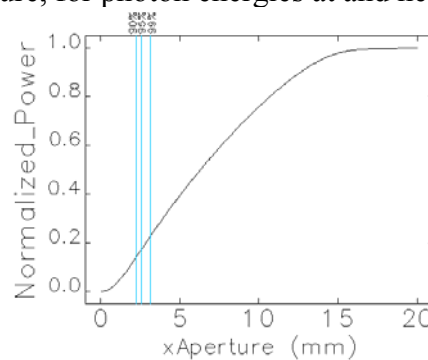


Figure 2-4: Transmitted x-ray power as function of square aperture sizes.

Figure 2-3 shows the flux of transmitted monochromatic x-ray photons within the central cone, plotted as a function of a square aperture width. Using the 245-eV curve because it has the most photons in the central cone, we obtain three aperture sizes: 2.25 mm, 2.80 mm, and 3.45 mm, corresponding to 90%, 95% and 99% of transmission efficiency, respectively. Figure 2-4 shows

the fraction of total x-ray power transmitted through the square aperture plotted as a function of the aperture width. We note that the same aperture that transmits 95% monochromatic photons at 245 eV will block approximately 80% total x-ray power.

2.2 Minimum K for horizontally polarized x-ray operations

Figure 2-5 shows an angle-integrated spectrum of IEX-EMU with $K_{y,\min} = 0.989$. At this setting, the first harmonic photon energy ω_1 is 2500 eV. A typical monochromator near 2450 eV, the location of the photon spectrum peak. Figure 2-6 shows the x-ray beam profiles from IEX-EMU at $K_{y,\min} = 0.989$ measured along x -axis (left panel) and y -axis (right panel): the total x-ray power profile, the monochromatic x-ray profiles at 2500 eV (first harmonic), 2475 eV, 2450 eV (near peak flux), and 2425 eV (normally unused), along with two lines indicating the proposed 2.5 mm square aperture.

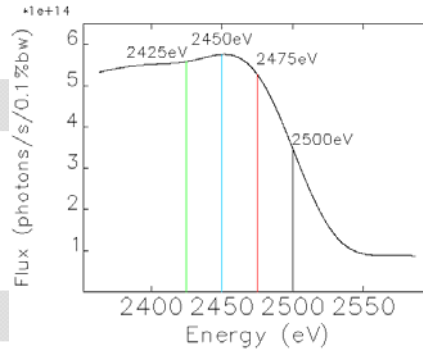


Figure 2-5: Monochromatic x-ray flux through a large pinhole at 20-m from IEX-EM undulator with $K = 0.989$ and the first harmonic energy of 2500 eV.

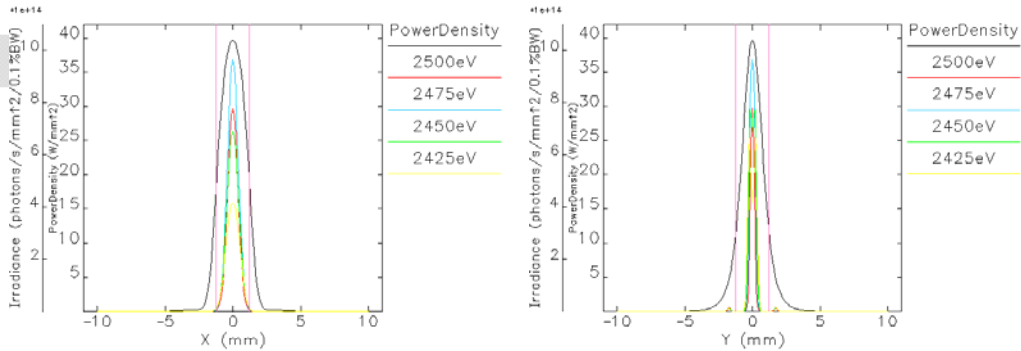


Figure 2-6: On-axis horizontal (left) and vertical (right) total x-ray power profiles of IEX-EM undulator with minimum K at 20 m from the source, along with monochromatic x-ray profiles at 2500 eV (first harmonic), 2475 eV, 2450 eV, and 2425 eV.

Comparing Figure 2-6 with Figure 2-2, we note the following:

- (1) While the power profile changed little in the vertical plane as expected, it is affected strongly by the K/γ ratio in the horizontal plane.
- (2) The monochromatic x-ray profiles in the horizontal plane also changes significantly for different K . At low- K settings, the first harmonic photon energy is high and the central cone is narrow, the x-ray profile is mainly determined by the horizontal e-beam

divergence. At high- K settings, the central cone is wider than the e-beam divergence, hence the x-ray profile reflects more feature of the radiation pattern.

- (3) The monochromatic x-ray profiles in vertical plane behave similarly to those in the horizontal plane, although the radiation patterns of the central cones are better preserved in for all K values since the e-beam divergence angle is smaller in the vertical plane.

Figure 2-7 shows the fraction of transmitted monochromatic x-ray photons within the central cone, plotted as a function of square aperture size. Compared with Figure 2-3, the mono beam is more compact at lower K and 99% photons will pass through the 2.5-mm square aperture. Figure 2-8 shows the fraction of total x-ray power transmitted through the aperture plotted as a function of the aperture size. We note that the 2.5-mm aperture intercepts only about 1/3 of total x-ray power. This should be sufficient to generate needed signals for beam position measurements. Since the total power is low with open gap, the downstream optics will not be overloaded even though the pass-through fraction is increased to 2/3.

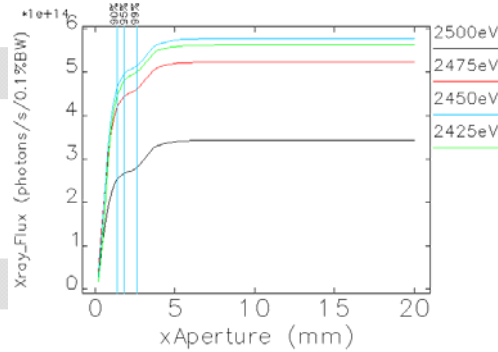


Figure 2-7: Monochromatic x-ray photon flux in the central cone plotted as a function of square aperture size, for photon energies at and near the first harmonic. The vertical lines are at 1.4, 2.0, and 2.7 mm, respectively.

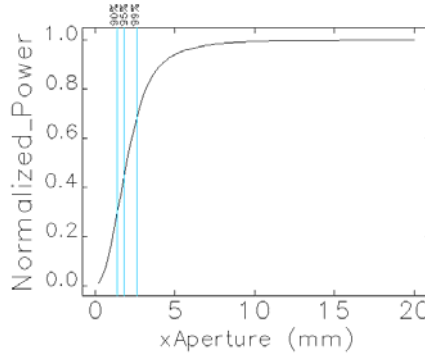


Figure 2-8: Transmitted x-ray power as function of square aperture size.

2.3 K -dependence of beam size and XBPM signal intensity for horizontally polarized x-rays

Now let us look at beam sizes when K takes values between its maximum and minimum. The left panel of Figure 2-9 shows the horizontal and vertical beam sizes (FWHM) of the x-ray power profiles. As expected, the horizontal beam size W_x exhibits a stronger dependence on undulator fields,

$$W_x = \frac{aS}{\gamma} (K^3 + b^3)^{1/3}, \quad (a = 1.683 \text{ and } b = 0.453), \quad (1)$$

where the aperture distance $S = 20$ m. The right panel of Figure 2-9 shows the vertical beam size W_y , which shows a very weak dependence on undulator fields,

$$W_y = \frac{cS}{\gamma} \left[1 + \left(\frac{K}{K_0} \right)^4 \right]^{1/4}, \quad (c = 1.306 \text{ and } K_0 = 7.98). \quad (2)$$

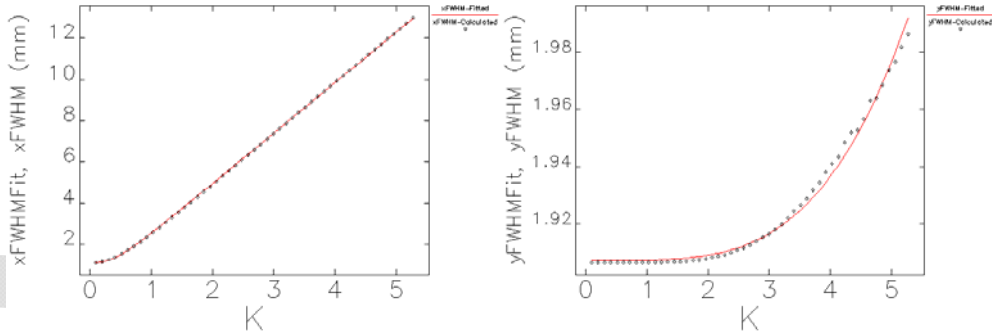


Figure 2-9: Projected horizontal and vertical profile sizes (FWHM) for IEX-EM undulators as a function of undulator field parameters.

Figure 2-10 shows the required aperture width to permit 90%, 95%, and 99% of the first harmonic monochromatic power through the square aperture. As K decreases, the first harmonic wavelength decreases, and the central cone size decreases. Except at the maximum K -settings, more than 99% of the monochromatic x-rays pass through the proposed 2.5-mm aperture.

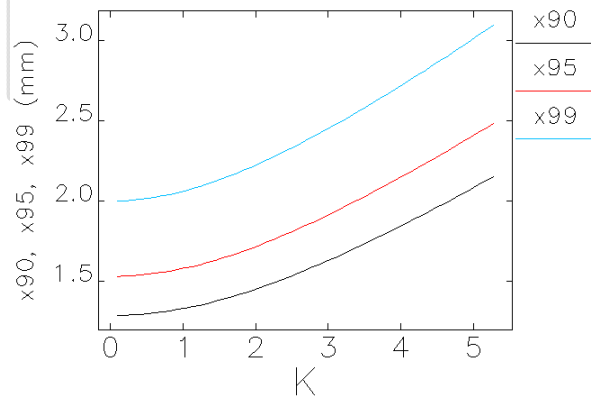


Figure 2-10: Required square aperture size for transmitting 90%, 95%, and 99% of the radiation in the first harmonic central cone.

To provide an estimate of the GRID-XBPM signal intensity, we used XOP to calculate the number of x-ray photons (listed in us.out) through the aperture ($1.25 \text{ mm} \leq x \leq 9.25 \text{ mm}$; $-5 \text{ mm} \leq y \leq 5 \text{ mm}$) and in the energy window ($9 \text{ keV} \leq \omega \leq 40 \text{ keV}$). From Figure 2-2, we can see that this aperture captures all photons impacting the XBPM on the right-hand-side. Figures 2-11 shows a typical spectrum passing through the aperture, where we can see that the photon flux is decreasing rapidly at the high-energy end and the choice of upper cutoff is not critical. Figure 2-12 shows the estimated XRF signal intensity where we have assumed an XRF

fluorescence efficiency of 44% for Cu and 0.001 sr solid angle for the detector. The self absorption was neglected due to grazing incidence. We note that at $K_{y,\min} = 0.989$, the XBPM signal is only 0.1% of its full-gap value.

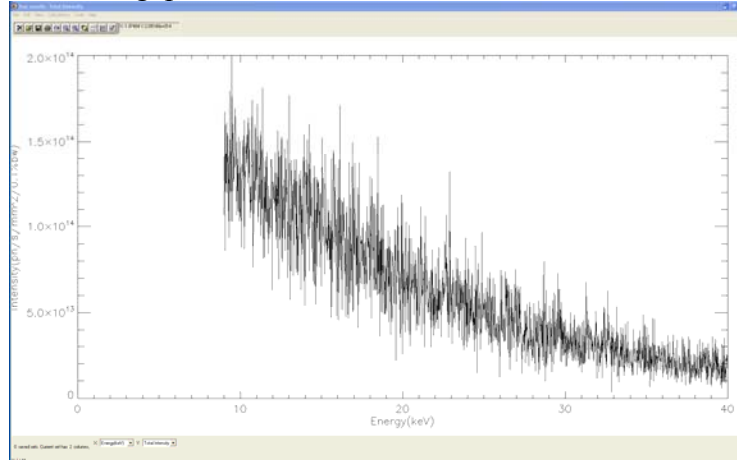


Figure 2-11: Spectrum of IEX-EMU ($K_y = 5.27$) x-rays passing through an aperture simulating the GRID-XBPM acceptance window: $\{1.25 \text{ mm} \leq x \leq 9.25 \text{ mm}; 0 \leq y \leq 5 \text{ mm}; 9 \text{ keV} \leq \omega \leq 40 \text{ keV}\}$.

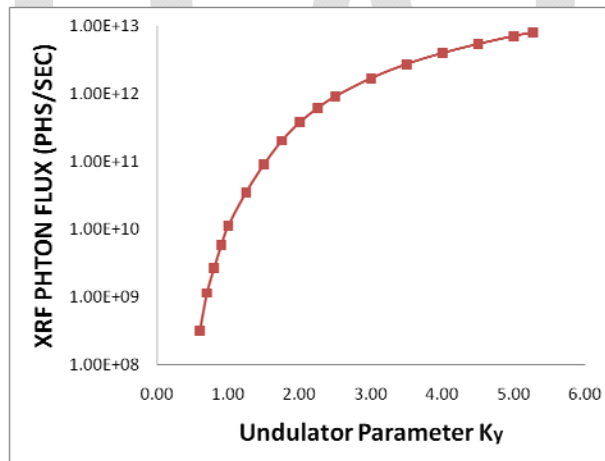


Figure 2-12: Estimated XRF signal intensity of one GRID-XBPM plate at +1.25 mm from the beam axis for the IEX-EM undulator to operate in horizontal polarization mode. The solid angle of the detector is assumed to be 0.001 sr.

3. Vertically polarized undulator beam properties

In this section, we calculate spectra and power density distributions for beams with linear polarization in the vertical plane and compare the patterns with a proposed aperture.

3.1 Maximum K for vertically polarized x-rays

Figure 3-1 shows an angle-integrated spectrum of the IEX-EMU for $K_{x,\max} = 3.86$. At this setting, the first harmonic photon energy ω_1 is 440 eV. The monochromatic x-ray user may set his monochromator near the peak of photon flux at approximately 431 eV.

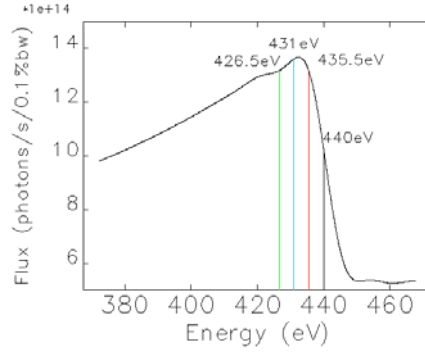


Figure 3-1: Monochromatic x-ray flux through a 5 mm × 5 mm aperture which encloses the central cone at 20-m from IEX-EMU with $K_x = 3.86$ and $\omega_1 = 440$ eV.

Figure 3-2 shows the IEX-EMU x-ray beam profiles measured along the x -axis (left panel) and y -axis (right panel): the total x-ray power profile, the monochromatic x-ray profiles at 440 eV (first harmonic), 435.5 eV, 431 eV (near peak flux), and 426.5 eV (normally unused). The maximum flux in Figure 3-1 corresponds to photon energy slightly below ω_1 with a wider opening angle than in Figure 3-2. The vertical lines indicate the proposed 2.5-mm square apertures.

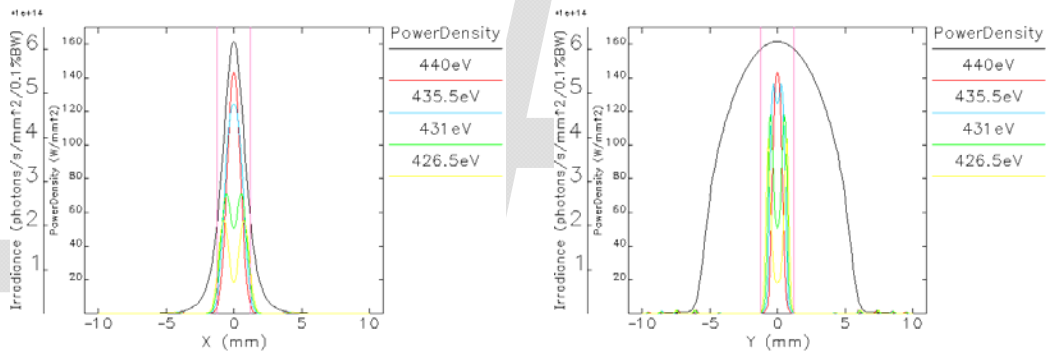


Figure 3-2: Calculated total x-ray power profiles 20 m from the IEX-EMU source ($K_x = 3.86$, $K_y = 0$), along with monochromatic x-ray profiles at 440 eV (first harmonic), 435.5 eV, 431 eV, and 426.5 eV. The left and right panels show the power densities measured on the x -axis and y -axis, respectively.

Figure 3-3 shows the fraction of transmitted monochromatic x-ray photons within the central cone, plotted as a function of width of a square aperture. Using the 431-eV curve because it has the most photons in the central cone, we obtain three aperture sizes: 1.95 mm, 2.25 mm, and 2.80 mm, corresponding to 90%, 95% and 99% of transmission efficiency, respectively. Figure 3-4 shows the fraction of total x-ray power transmitted through the square aperture plotted as a function of the aperture width. We note that the same aperture that transmits 95% monochromatic photons at 431 eV will intercept approximately 80% total x-ray power.

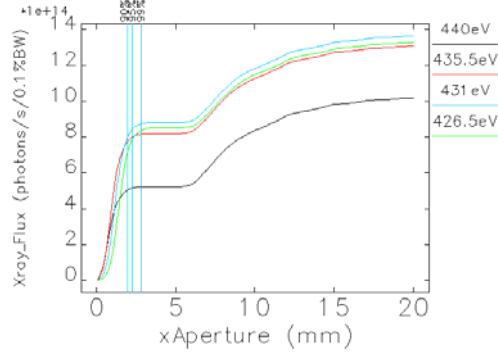


Figure 3-3: Monochromatic x-ray photon flux in the central cone plotted as a function of sides of square beam aperture, for photon energies at and near the first harmonic.

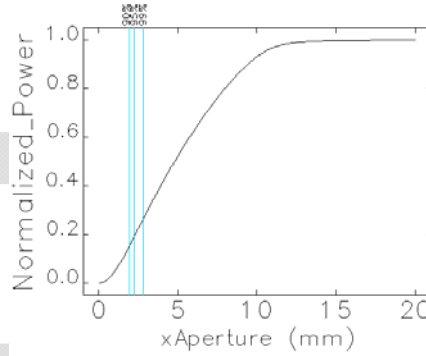


Figure 3-4: Transmitted x-ray power as function of square aperture sizes.

3.2 Minimum K for vertically polarized x-rays

Figure 3-5 shows an angle-integrated spectrum of IEX Undulator with $K_{x,\min} = 0.989$. At this setting, the first harmonic photon energy ω_1 is 2500 eV, and this plot is identical with Figure 2-5, except for the polarization of the x-ray photons. Figure 3-6 shows the beam profiles from IEX-EMU at $K_{x,\min} = 0.989$ measured along x -axis (left panel) and y -axis (right panel): the total x-ray power profile, the monochromatic x-ray profiles at 2500 eV (first harmonic), 2475 eV, 2450 eV (near peak flux), and 2425 eV (normally unused). An aperture of 2.5 mm, indicated by the vertical lines, would enclose essentially the entire central cone while blocking a good part of total x-ray power. Comparing Figures 3-6 and 3-2, we may make the following observations:

- (1) While the vertical power profile changed significantly with the K_x/γ , the horizontal power profile is nearly unchanged, as one may expect.
- (2) The horizontal monochromatic x-ray profiles changed significantly for different K . At low- K settings, the first harmonic photon energy is high and the central cone is narrow, the x-ray profile is mainly determined by the horizontal e-beam divergence. At high- K settings, the central cone radius is larger than the e-beam divergence angle, hence the x-ray profile is somewhat smeared by the e-beam divergence.
- (3) The vertical monochromatic x-ray profiles behave similarly to those in the horizontal plane, although the radiation patterns of the central cones is more distinct K since the e-beam divergence angle is smaller in the vertical plane.

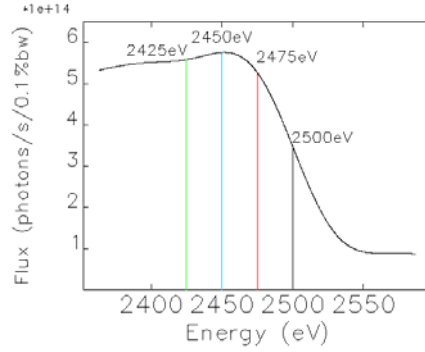


Figure 3-5: Monochromatic x-ray flux through a 5 mm × 5 mm aperture at 20-m from IEX-EMU with $K = 0.989$ and the first harmonic energy of 2500 eV.

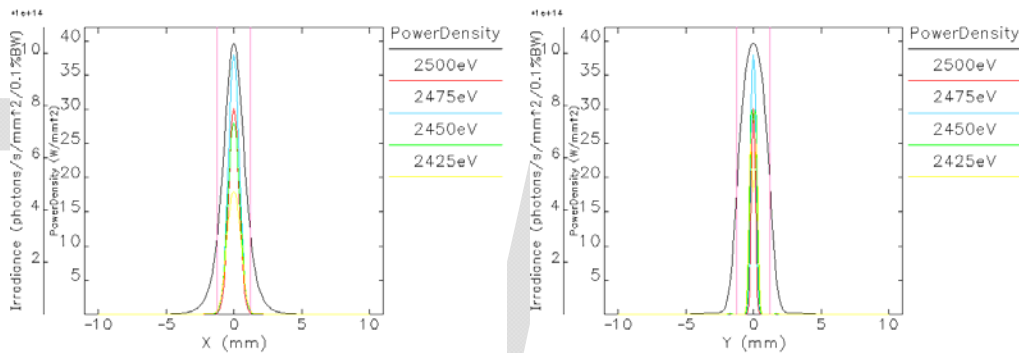


Figure 3-6: On-axis horizontal (left) and vertical (right) total x-ray power profiles of IEX-EMU at 20 m from the source point, along with monochromatic x-ray profiles at 2500 eV (first harmonic), 2475 eV, 2450 eV, and 2425 eV.

Figure 3-7 shows the fraction of transmitted monochromatic x-ray photons within the central cone, plotted as a function of square aperture size. Compared with Figure 3-3, the mono beam is more compact at lower K and 99% photons will pass through the 2.5-mm aperture. The same Figure 2-8 shows the fraction of total x-ray power transmitted through the aperture plotted as a function of the aperture size, from which we knew that the 2.5-mm aperture intercepts about 1/3 of the total x-ray power.

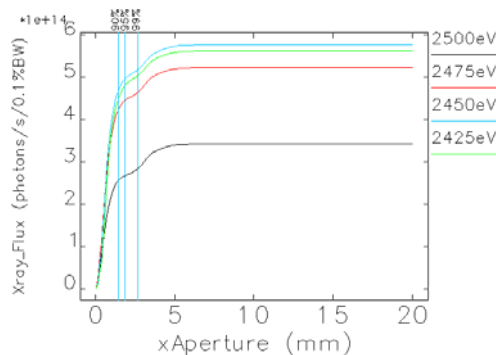


Figure 3-7: Monochromatic x-ray photon flux in the central cone plotted as a function of square aperture size, for photon energies at and near the first harmonic.

3.3 K -dependence of beam size and XBPM signal intensity for vertically polarized x-rays

The left and right panels of Figure 3-8 shows the horizontal and vertical beam sizes (FWHM) of the x-ray power profiles, respectively. As expected, they are identical with Figure 2-8, except for exchanging plots of horizontal and vertical planes. The vertical beam size W_y is given by,

$$W_y = \frac{aS}{\gamma} (K^3 + b^3)^{1/3}, \quad (a = 1.683 \text{ and } b = 0.453); \quad (3)$$

and the horizontal beam size W_x is given by,

$$W_x = \frac{cS}{\gamma} \left[1 + \left(\frac{K}{K_0} \right)^4 \right]^{1/4}, \quad (c = 1.306 \text{ and } K_0 = 7.98). \quad (4)$$

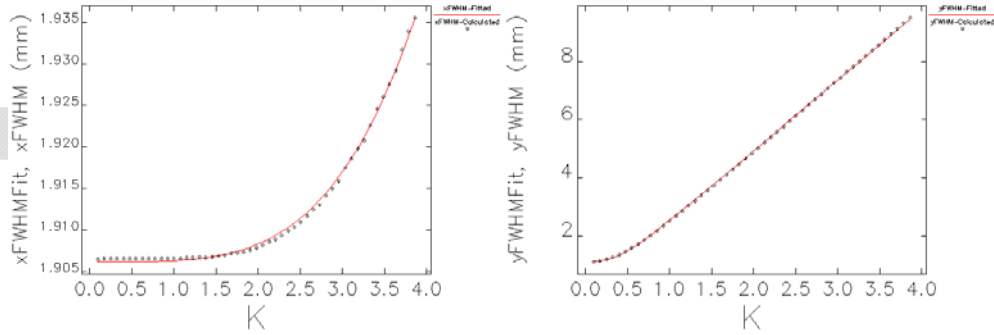


Figure 3-8: Projected horizontal and vertical profile sizes (FWHM) for IEX-EM undulators as a function of undulator field parameters.

Figure 3-9 shows the required aperture width to permit 90%, 95%, and 99% of the first harmonic monochromatic power through the square aperture. As K decreases, the first harmonic wavelength decreases, and the central cone size decreases. Only at the maximum K -settings less than 95% of the monochromatic x-rays pass through the proposed 2.5-mm aperture.

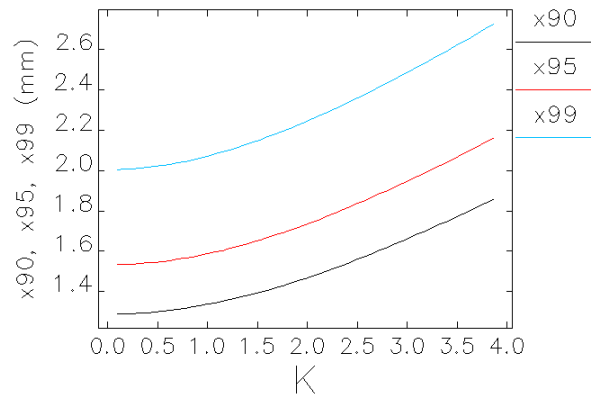


Figure 3-9: Required square aperture size for transmitting 90%, 95%, and 99% of the radiation in the first harmonic central cone.

To provide an estimate of the GRID-XBPM signal intensity, we used XOP to calculate the number of x-ray photons through the aperture ($1.25 \text{ mm} \leq x \leq 9.25 \text{ mm}$; $-7 \text{ mm} \leq y \leq 7 \text{ mm}$) and in the energy window ($9 \text{ keV} \leq \omega \leq 40 \text{ keV}$). From Figure 3-2, we can see that this aperture

captures all photons impacting the XBPM on the right-hand-side. Figure 3-10 shows the estimated XRF signal intensity assuming an XRF fluorescence efficiency of 44% for Cu and a solid angle 0.001 sr for the detector. At $K_{y,\min} = 0.989$, the XBPM signal is only 0.1% of its full-gap value. Comparing Figures 2-12 and 3-11, we can see that for the same K -values, the XBPM signal is typically 10 – 30 times weaker in the vertical polarization mode, probably because the spectrum of off-plane wiggler radiation is softer.

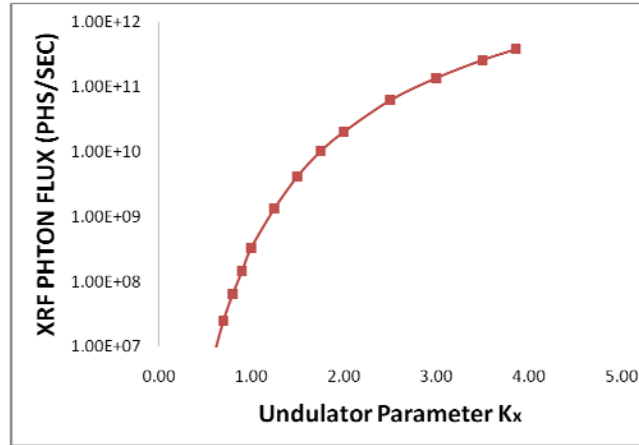


Figure 3-10: Estimated XRF signal intensity of one GRID-XBPM plate at +1.25 mm from the beam axis for the IEX-EM undulator to operate in vertical polarization mode. The solid angle of the detector is assumed to be 0.001 sr.

4. Circularly polarized undulator beam properties

In this section, we calculate spectra and power density distributions for beams with perfect circular polarization. Since the maximum power density is found off axis, the power distributions are expected to be dramatically different.

4.1 Maximum K for circularly polarized x-rays

Figure 4-1 shows an angle-integrated spectrum of the IEX-EMU in circular polarization mode for $K_x = K_y = 2.73$. At this setting, the first harmonic photon energy ω_1 is 440 eV. The monochromatic x-ray user may set his monochromator near the peak of photon flux at approximately 431 eV.

Figure 4-2 shows the IEX-EMU x-ray beam profiles measured along the x -axis (left panel) and y -axis (right panel): the total x-ray power profile, the monochromatic x-ray profiles at 440 eV (first harmonic), 435.5 eV, 431 eV (near peak flux), and 426.5 eV (normally unused). The maximum flux in Figure 4-1 corresponds to photon energy slightly below ω_1 with a wider opening angle than in Figure 4-2. The vertical lines indicate the proposed 2.5-mm square apertures.

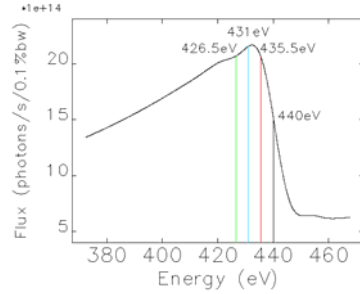


Figure 4-1: Monochromatic x-ray flux through a 5 mm × 5 mm aperture which encloses the central cone at 20-m from IEX-EMU with $K_x = K_y = 2.73$ and $\omega_1 = 440$ eV.

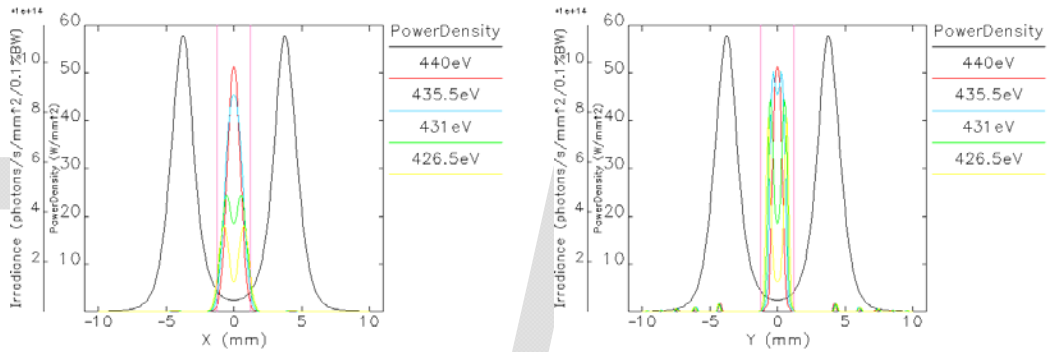


Figure 4-2: Calculated total x-ray power profiles 20 m from the IEX-EMU source in circular polarization mode ($K_x = K_y = 2.73$), along with monochromatic x-ray profiles at 440 eV (first harmonic), 435.5 eV, 431 eV, and 426.5 eV. The left and right panels show the power densities measured on the x-axis and y-axis, respectively.

Figure 4-3 shows the fraction of transmitted monochromatic x-ray photons within the central cone, plotted as a function of width of a square aperture. Using the 431-eV curve because it has the most photons in the central cone, we obtain three aperture sizes: 1.4 mm, 2.0 mm, and 2.7 mm, corresponding to 90%, 95% and 99% of transmission efficiency, respectively. Figure 4-4 shows the fraction of total x-ray power transmitted through the square aperture plotted as a function of the aperture width. We note that very little power passes through the aperture in the circular polarization mode. We will no longer concern us with transmitted power for circularly polarized x-ray operations.

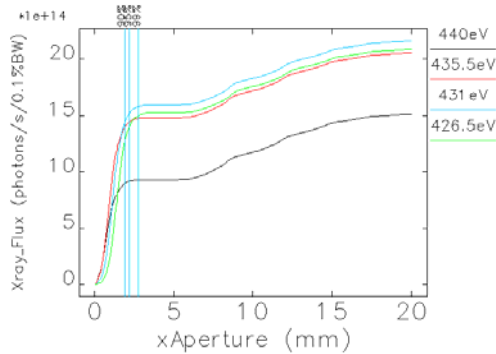


Figure 4-3: Monochromatic x-ray photon flux in the central cone plotted as a function of sides of square beam aperture, for photon energies at and near the first harmonic.

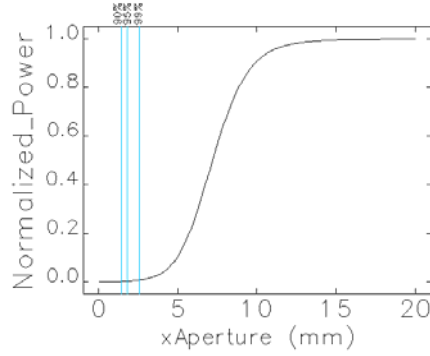


Figure 4-4: Transmitted x-ray power as function of square aperture sizes.

4.2 Minimum K for circularly polarized x-rays

Figure 4-5 shows an angle-integrated spectrum of IEX-EMU with $K_x = K_y = 0.699$. At this setting, the first harmonic photon energy ω_1 is 2500 eV. Figure 4-6 shows the x-ray beam profiles from IEX-EMU ($K_x = K_y = 0.699$) measured along x -axis (left panel) and y -axis (right panel): the total x-ray power profile, the monochromatic x-ray profiles at 2500 eV (first harmonic), 2475 eV, 2450 eV (near peak flux), and 2425 eV. An aperture of 2.5 mm is indicated by the vertical lines. Comparing Figure 4-6 with Figure 4-2, we can make the following observations:

- (1) The power profile changed dramatically from a donut shape at high field shrinking down to a single peak at low field.
- (1) The horizontal monochromatic x-ray profiles changed significantly for different K . At low- K settings, the first harmonic photon energy is high and the central cone is narrow, the x-ray profile is mainly determined by the horizontal e-beam divergence. At high- K settings, the central cone radius is larger than the e-beam divergence angle, hence the x-ray profile is somewhat smeared by the e-beam divergence.
- (2) The vertical monochromatic x-ray profiles behave similarly to those in the horizontal plane, although the radiation patterns of the central cones is more distinct at lower K since the e-beam divergence angle is smaller in the vertical plane.

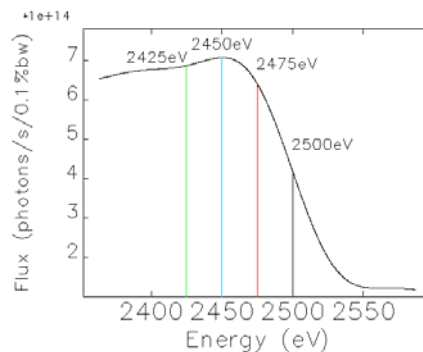


Figure 4-5: Monochromatic x-ray flux through a 5 mm \times 5 mm aperture at 20-m from IEX-EMU with $K_x = K_y = 0.699$ and the first harmonic energy of 2500 eV.

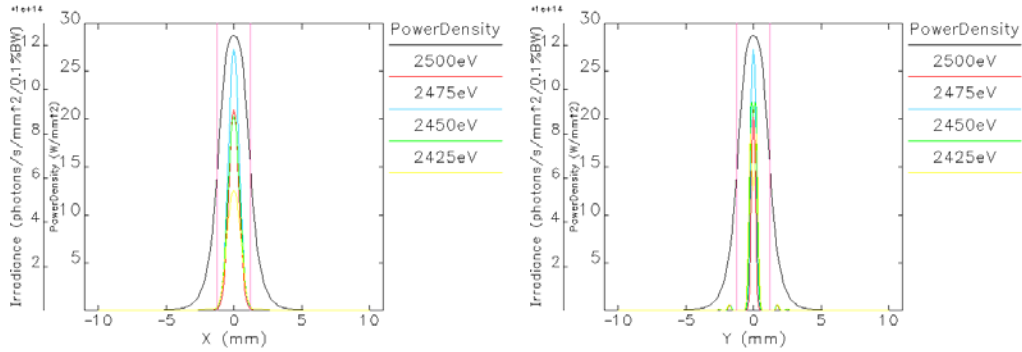


Figure 4-6: On-axis horizontal (left) and vertical (right) total x-ray power profiles at 20 m from the of IEX-EMU source ($K_x = K_y = 0.699$), along with monochromatic x-ray profiles at 2500 eV (first harmonic), 2475 eV, 2450 eV, and 2425 eV.

Figure 4-7 shows the fraction of transmitted monochromatic x-ray photons within the central cone, plotted as a function of square aperture size. Compared with Figure 4-3, the mono beam is more compact at lower K and 98% photons will pass through the 2.5-mm aperture.

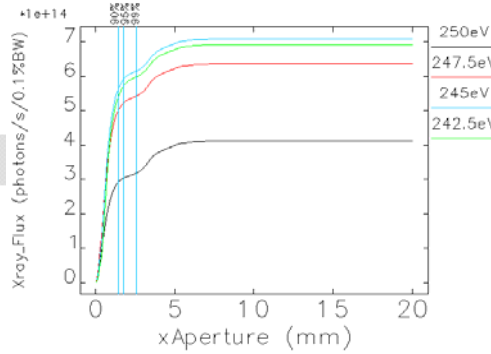


Figure 4-7: Monochromatic x-ray photon flux in the central cone plotted as a function of square aperture size, for photon energies at and near the first harmonic.

4.3 K-dependence of beam size and XBPM signal intensity for circularly polarized x-rays

Figure 4-8 shows the required aperture width to permit 90%, 95%, and 99% of the first harmonic monochromatic power through the square aperture. As K decreases, the first harmonic wavelength decreases, and the central cone size decreases. Only at the maximum K -settings less than 99% of the monochromatic x-rays pass through the proposed 2.5-mm aperture.

To provide an estimate of the GRID-XBPM signal intensity, we used XOP to calculate the number of x-ray photons through an aperture ($1.25 \text{ mm} \leq x \leq 9.25 \text{ mm}$; $-7 \text{ mm} \leq y \leq 7 \text{ mm}$) and in an energy window ($9 \text{ keV} \leq \omega \leq 40 \text{ keV}$). From Figure 4-2, we can see that this aperture captures all photons impacting the XBPM on the right-hand-side. Figure 4-9 shows the estimated XRF signal intensity using an XRF fluorescence efficiency of 44% for Cu and a solid angle 0.001 sr for the detector. At $K_x = K_y = 0.699$, the XBPM signal is only 0.1% of its full-gap value. Comparing Figures 2-12 and 3-11, we can see that for the same K -values, the XBPM signal is typically 10 – 30 times weaker in the vertical polarization mode, probably due to the softer spectra of the off-plane wiggler radiation.

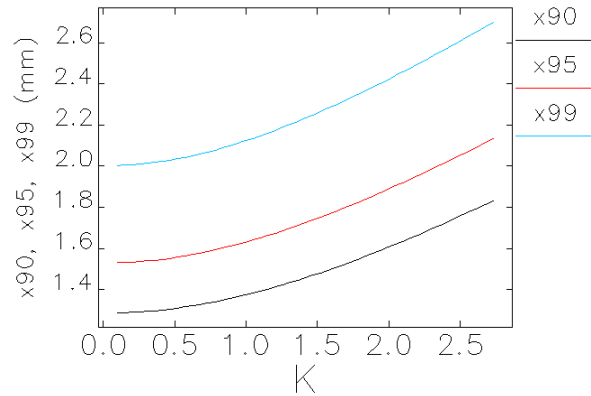


Figure 4-8: Required square aperture size for transmitting 90%, 95%, and 99% of the radiation in the first harmonic central cone.

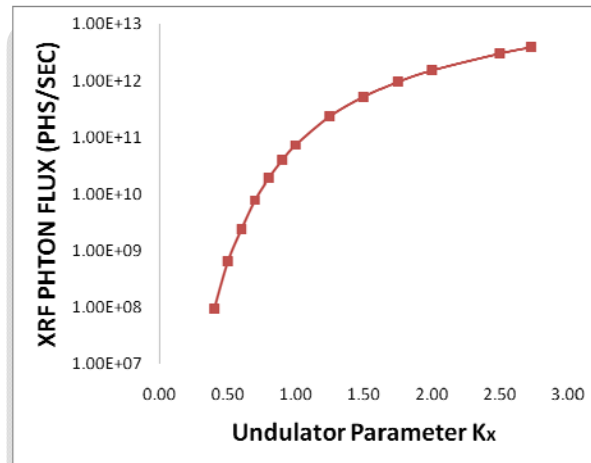


Figure 4-9: Estimated XRF signal intensity of one GRID-XBPM plate at +1.25 mm from the beam axis for the IEX-EM undulator to operate in circular polarization mode. The solid angle of the detector is assumed to be 0.001 sr.

5. Discussions and conclusions

We calculated the x-ray profiles of the intermediate-energy x-ray (IEX) beamline's electromagnetic undulator (EMU) at 20 m from the source point and compared them with a proposed 2.5 mm square aperture for the grazing-incidence insertion device x-ray beam position monitor (GRID-XBPM). The transmission efficiency of the central cone is a function of undulator field parameter K . For small K -values, 99% of the monochromatic x-ray photons in the central cone pass through the proposed 2.5 mm square aperture. For large K -values, the transmission efficiency decreases as the central cone expands. In the worst case of $K_y = 5.27$, over 90% of the monochromatic x-ray photons in the central cone still pass through the aperture.

Enlarging the aperture from the Undulator A's small aperture of 2 mm (H) \times 1.5 mm (V) to 2.5 mm square has strong impact on the XBPM signal. Figure 5-1 shows an estimate of the x-ray fluorescence signal level as a function of field parameter K : The strongest signal for horizontally

polarization mode ($K_y = 5.27$) is 3×10^4 times higher than the weakest signal for vertically polarization mode ($K_x = 0.99$).

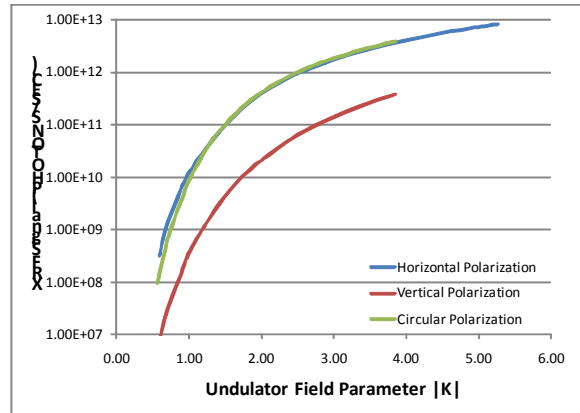


Figure 5-1: Estimated XRF signal intensity from one GRID-XBPM plate at +1.25 mm from the beam axis of the IEX-EMU, plotted as a function of K for horizontally, vertically, and circularly polarized x-ray operations.

[References]

- [1] Bingxin Yang and Glenn Decker, A Concept for Grazing Incidence XBPM in APS Front Ends, APS/ASD/DIAG Technote DIAG-TN-2009-009.
- [2] B.X.Yang, G. Decker, S. H. Lee, and P. Den Hartog, High-power hard x-ray beam position monitor development at the APS, BIW10, Santa Fe, 2010.
- [3] B.X.Yang and K. Schlax, "Undulator-A X-ray Profile Calculations for Grazing Incidence XBPM Design," ANL/APS/ASD/DIAG tech notes, DIAG-TN-2010-008, July, 2010.
- [4] R. Dejus, M. Jaski, and S. Sasaki, "On the selection of undulator for the IEX beamline: power and spectral performance," ANL/APS/ASD/MD tech note, MD-TN-2009-003, March 20, 2009.
- [5] R. Dejus, private communication, email to Bingxin Yang dated July 8, 2010.
- [6] M. Sánchez del Río and R. J. Dejus, "Status of XOP: an x-ray optics software toolkit," SPIE Proc. 5536, 171-174 (2004).
- [7] H. Shang, private communications.
- [8] XOP 2.3, ESRF web site, downloaded May 17, 2010.